ADDIS ABABA UNIVERSITY

ADDIS ABABA INSTITUTE OF TECHNOLOGY

SCHOOL OF MULTIDISCIPLINARY ENGINEERING

CENTER FOR MATERIALS ENGINEERING

MASTER THESIS

Investigation of 2D Hexagonal Transition Metal Dichalcogenide Heterostructures for Photocatalytic Water Splitting and Photovoltaic Solar Cells Using Density Functional Theory

By: BEREKET FEKEDE ANANKO

A Thesis Submitted to the Center for Materials Engineering in Partial Fulfillment of the Requirements for the Degree of Science in Materials Engineering

March 2025

This is to certify that the thesis entitled "**Investigation of 2D Hexagonal Transition Metal Dichalcogenide Heterostructures for Photocatalytic Water Splitting and Photovoltaic Solar Cells Using Density Functional Theory**, as a partial fulfillment of the Master of Science in Materials Engineering degree requirements, it is prepared and submitted by Bereket Fekede in accordance with the university's regulations and the acknowledged standards of quality and originality**.**

Approval by the Board of Examiners

Goergis Alene Asres (Dr.)	signature	Date
Advisor	_____	_____
Kingsley Obodo (Dr.)		
Co Advisor	_____	_____
Anteneh Wedajo (Dr .)		
Internal Examiner	_____	_____
Aman Kassa (Dr.)		
External Examiner	_____	_____

DECLARATION

I hereby declare that the work that is being presented in this thesis entitled "**Investigation of 2D Hexagonal Transition Metal Dichalcogenide Heterostructures for Photocatalytic Water Splitting and Photovoltaic Solar Cells Using Density Functional Theory**" has significance to me, has not been submitted for a degree at any other institution, and all the resources utilized in this thesis have been appropriately acknowledged.

Name: Bereket Fekede Ananko signature Date

_____ _____

This is to confirm that the candidate's declaration above is accurate to the best of our knowledge and has been submitted for the examination with our approval as university advisor.

Goergis Alene Asres (Dr) signature Date

Advisor _____ _____

ACKNOWLEDGMENT

I want to thank God for allowing me to complete my master's degree and thesis. Next, I would like to express my gratitude to Dr. Georgies Alene, my adviser, for his guidance, inspiration, and continuous support during the writing of my master's thesis. I also want to thank Dr. Kingsley Obodo, my coadviser, for his unwavering support and the priceless CHPC supercomputer resources he provided for intricate computations. Without it, I could not have finished my thesis. And I want thanks center for Material Engineering Department and Addis Ababa University for the female scholarship I had rewarded for all this years. Finally, I would want to express my gratitude to my friends and family for their great assistance in completing my thesis. You're always accessible, Thank you!!

Abstract

Advances in materials science and technology are critical to the development of different sophisticated processes. It is imperative to recognize the significance of affordable, sustainable, and eco-friendly energy alternatives. Significant scientific and technological interest has consistently been shown in the use of hydrogen-based technologies towards the provision of clean, green energy in the energy mix. The formation of heterostructures combining MoS_2, WS_2, and ReS_2 is a promising strategy in developing 2D semiconductor-based photo-catalysts for water splitting. This specific Research paper involves theoretical simulations to predict and optimize the properties of MoS_2, WS_2, and ReS_2 heterostructures. This approach helps in understanding the fundamental mechanisms at play and designing more effective photo-catalytic systems. Monolayers and heterostructure combining MoS_2, WS_2, and ReS_2 is constructed and investigated in this study using Density functional study as implemented in quantum ESPRESSO and CASTEP. ReS_2 -WS_2 hetero structure is type II hetero junction which has greater energy level than that of WS_2 monolayer. It is also demonstrated appropriate CBM position located within -2.650 to -4.010eV range according to the band alignment, highlighting another class of suitable materials for hydrogen evolution reaction. In similar manner, hetero structure ReS_2-MoS_2 has greater energy level than MoS_2 monolayer. The band alignment is shows us appropriate CBM position located within -3.054 to -4.350 eV range, this denote this hetero structure is suitable for hydrogen production. The power conversion efficiency of MoS_2, WS_2 and MoS_2 –WS_2 heterostructure is computed, and the results exhibit high efficiency with values of 18.7%, 17.0% and 21.4%, respectively making these materials promising for photovoltaic solar cell.

Keywords: DFT, band alignment, band gap, power conversion efficiency, photo-voltaic, photo-catalyst, water splitting

Table of Contents

List of Figures

List of table

Chapter 1: Introduction

1.1 Background and Motivation

The development of sustainable energy infrastructure is a new field that is being studied to control the world's energy consumption in light of population growth, sharing of renewable energy sources, and per-capita energy consumption. To reach the 2030 energy objectives, the infrastructure and energy technologies that are in place now must be reinforced. This area of materials science and engineering is crucial and expanding quickly that improved functional materials for energy-related devices. [1] However, the deployment of these intermittent renewable energy sources has been limited by the difficulties associated with energy storage and integration into the present power system. Hydrogen is an energy vector which possessing a high energy density and potential which is carbon neutral that can be stored by water splitting techniques including electrochemical and photo-electrochemical processes. Hydrogen can be used as a sustainable energy source, similar to wind and solar power. [2-4]

One of the biggest challenges facing humankind is providing cheap, clean energy to a growing global population. [5] By 2040, the world's energy consumption is expected to have increased from 17 TW in 2010 to 27 TW. The world's energy supply is still dominated by fossil fuels, but growing worries about how human-caused carbon dioxide is affecting the environment make renewable energy sources like solar and wind more appealing. [6-9] However, the vast majority of the earth's energy resources come from non-renewable sources including nuclear energy, oil, coal, and natural gas, and their supplies are finite. When these fossil fuels are used, they produce energy through burning, but at the same time, a number of serious environmental issues such water pollution, greenhouse gas emissions, global warming, and the formation of an ozone hole arise. As a result, many scientists, policy makers, and organizations are motivated to look for fresh, sustainable sources of alternative energy. [10]

One alternative energy source can be by splitting water and producing hydrogen. However, significant development in technology is required before water splitting can be widely used in an economically viable manner. The creation of very active, stable electro-catalysts made of elements that are readily available on Earth is one essential need. [11] Because of its promise in a wide range of technological applications, the application and usage of 2D materials is a topic that is consistently receiving substantial research interest. [12–21]

Our globe receives a tremendous amount of energy from the sun every day, and this source has garnered significant interest as a potential substitute for fossil fuels in order to reduce greenhouse gas emissions and supply energy for present and future human needs. A more attractive strategy would be to use photo-catalytic processes to synthesize transportable and storable chemical fuels. These processes use solar energy to create

molecular bonds, which are then stored as energy through a thermodynamic "uphill reaction" [22]
Numerous photocatalysts have been created for solar energy conversion and environmental protection since Fujishima and Honda discovered the photocatalytic splitting of water on TiO_2 electrodes in 1972. [23] The process of photocatalysis is mediated by semiconductors. Semiconductors, which consist of an empty conduction band (CB) and a full valence band (VB), are able to absorb light and use it for chemical processes. Examples of these semiconductors are TiO_2, [24], CdS, [25], and $BiVO_4$, [26], among others. [27]

Light irradiation can lead to the formation and separation of electron-hole pairs. The photogenerated electrons and holes can be employed as reductants or oxidants to achieve water reduction or pollutant degradation, respectively. [28] The poor activity of semiconductor photocatalysts is caused by the unstable and readily recombined photogenerated electrons and holes in the excited states. [29]
A viable method for producing H_2 from solar energy that is inexpensive, clean, and ecologically acceptable is photocatalytic water splitting. The photocatalytic water splitting procedure has three essential stages: the extraction of solar light, the separation and transfer of charges, and the catalytic reactions for the evolution of H_2 and O_2.

In 1972, Honda and Fujishima discovered the photoelectrochemical (PEC) water-splitting on a titania electrode. Since then, photocatalysts have become a viable method for converting solar energy into clean, carbon-neutral H_2 fuel in a low-cost and ecologically beneficial manner. [30]

A good catalyst can assist minimize the energy needed for the uphill reaction of water splitting, which takes 237 kJ/mol to occur. Reduction and oxidation processes take place at the catalyst's surface during the water splitting process. In general, water splitting is the process of dividing water into hydrogen and oxygen in a 2:1 ratio with the aid of suitable photocatalysts. Water splitting by photocatalysis has a well-established mechanism. [31] An energy-appropriate photon is absorbed to start the reaction, excitining electrons from the valence band maximum (VBM) to the conduction band minimum (CBM). The generated electron-hole pairs go to the photocatalyst's surface when they have the right potentials—the valence band maximum (VBM) being more positive than the water oxidation potential and the conduction band minimum (CBM) being more negative than the H+/H2 redox potential. Electrons at the surface active sites convert water to hydrogen, whereas holes oxidize water to produce oxygen. [32]

Scientists directed their attention to two-dimensional (2D) stacked materials after learning about graphene. The layered crystal structure of 2D materials is characterized by layers that are held together by weak van der Waals (vdW) force and strong covalent in-plane bonding. [33] The development of this technology has enabled research on the creation, manufacturing, and use of two-dimensional materials. Although several heterostructures are anticipated to be feasible choices for producing high-performance solar materials, their efficiency is still below the target level. Research into different 2D

hetero-structure materials is therefore essential to better understand their characteristics and discover more effective materials that can yield remarkable effects across the interface. [34]

Advances in materials science and technology are critical to the development of different sophisticated processes. It is imperative to recognize the significance of affordable, sustainable, and eco-friendly energy alternatives. Significant scientific and technological interest has consistently been shown in the use of hydrogen-based technologies towards the provision of clean, green energy in the energy mix. [35]

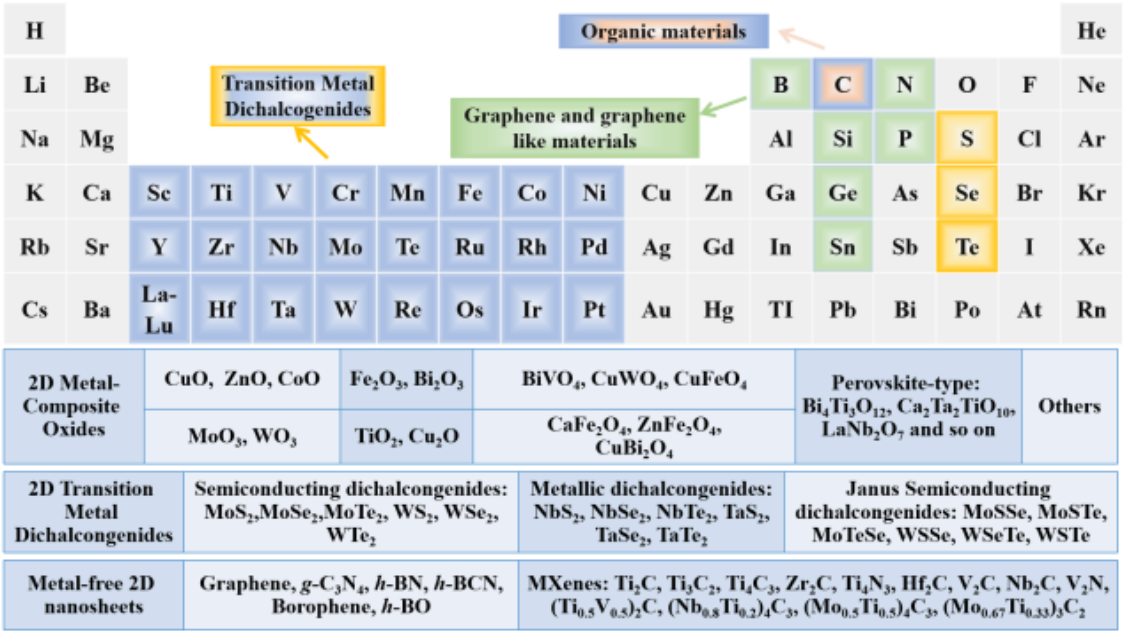

Figure 1 . Periodic table with highlighted elements for typical ultrathin 2D materials [36]

It is generally known that the TMDs showed layered compounds with the common chemical formula MX2, where X is a chalcogen atom (S, Se, and Te) and M is a transition metal from group IV/V/VI (Ti, Zr, Hf, V, Nb, Ta, Mo, and W). [37] Three atomic layers make up each TMD monolayer, with the M layer positioned between two chalcogen layers.

In their discussion of the latest developments and potential applications of ultrathin 2D semiconductor-based photo-catalysts for water splitting, Xiaoyong Yang et al. emphasize the importance of stable, affordable, and earth-abundant 2D semiconductor-based photo-catalysts. It also emphasizes the significance of creating precise theoretical models and comprehending charge transfer mechanisms. This thorough review discusses the state-of-the-art in 2D semiconductor-based photo-catalysts today and emphasizes the opportunities and difficulties in this quickly developing sector. [38]

1.2 Problem Statement

The fabrication and characterization of TDMs heterostructures for photo-catalytic applications provide a number of difficulties for researchers. These consist of repeatability, scalability, interface quality, and layer uniformity and control. For practical applications, reproducibility is essential since minor adjustments to the synthesis conditions might result in notable changes in the characteristics of the heterostructures. To enhance these processes and increase the usefulness of TDMs heterostructures in photo-catalytic water splitting and other energy-related applications, a multidisciplinary strategy involving materials science, chemistry, and engineering is required.

The formation of heterostructures combining MoS_2, WS_2, and ReS_2 is a promising strategy in developing 2D semiconductor-based photo-catalysts for water splitting. These structures leverage the unique properties of each material to enhance photo-catalytic performance, particularly in terms of light absorption, charge separation, and catalytic activity.

Key aspects of these heterostructures include enhanced light absorption, improved charge separation and transfer, synergistic effects, multiple active sites for hydrogen evolution reaction (HER) and oxygen evolution reaction (OER), enhanced stability and durability, and advanced fabrication techniques like layer-by-layer assembly.

This specific Research paper involves theoretical simulations to predict and optimize the properties of MoS2, WS2, and ReS2 monolayer and their heterostructures. This approach helps in understanding the fundamental mechanisms at play and designing more effective photo-catalytic systems.

In summary, the formation of heterostructures combining MoS_2, WS_2, and ReS_2 is a promising area of research in the field of photo-catalysis, offering potential improvements in light absorption, charge dynamics, and catalytic activity, which are essential for efficient Hydrogen evolution reaction. The combination of these materials may lead to enhanced stability under operational conditions, with less degradation than individual components.

1.3 Research Objectives

General Objective

To investigate 2D hexagonal transition metal dichalcogenide monolayer and their heterostructures of MoS_2-WS_2, ReS_2-WS_2 and ReS_2-MoS_2 as a candidate material for photocatalytic water splitting and photovoltaic applications.

Specific Objectives

-

- To optimize electronic properties of MoS_2, $WS_2$and ReS_2 monolayers
- To analyze the band structureand density of states of MoS_2-WS_2, ReS_2-WS_2, and ReS_2-MoS_2 heterostructures.
- To cvaluate the band edge values relative to water redox potential for hydrogen evolution reaction feasibility.
- To determine the power conversion efficiency for photovoltaic applications.

1.4 Thesis Structure

An over view of the related literature on two dimensional materials and TMDS, with Photo –catalytic water splitting and photovoltaic solar cells is presented in chapter 2. The key points of Theoretical background and computational methods considering Density Functional theory and Simulation parameter is covered in Chapter 3. Research objective, Background and motivation were described in Chapter 1. In Chapter 4 result and discussion covered that shows the construction of hetero-structure. Electronics properties of monolayers and hetero-structures including band structure, Density of state and Band edge alignment presented and Power conversion efficiency and photo catalytic water splitting covered. The comparative analysis and Challenges including recommended future work is discussed and Finally, summary of finding and recommendation of the thesis be presented in Chapter 5.

Chapter 2: Literature Review

2.1 Two-Dimensional Materials and TMDs

Dean CR and colleagues [39] have made significant advances in the realm of 2D materials. They published in 2010 the first 2D heterostructure (graphene/h-BN) to be atomically thin. 2D heterostructures made out of several MX_2 layers that are atomically thin have drawn a lot of interest very fast.[40] [41] Because van der Waals interactions between MX_2 layers, in which M represents the transition metal from group IV/V/VI (Ti, Zr, Hf, V, Nb, Ta, Mo and W), and X shows a chalcogen atom (S, Se, and Te) prevent dangling bonds from forming on the basal plane, the layers can form a variety of vertical or lateral heterostructures. Negative differential resistance (NDR) and interlayer excitons—properties that are unique to heterostructures built on MX_2 layers and absent from individual MX_2 layers—have been demonstrated. [42] [43] Furthermore, the hetero-structures of semiconducting MX_2 layers provide up fascinating opportunities for creating new and useful devices including p-n diodes and tunneling field effect transistors. MX_2 hetero-structures provide a fresh avenue for investigating novel devices and physics. [44] [45]

The application of 2D nanomaterials for photocatalytic hydrogen generation is discussed by Priyanka Ganguly et al., who also highlight current advancements in this field. [46] The production of 2D nanomaterials and their potential for applications involving surfaces are also covered. By offering a sizable surface area for catalytic activity, improving charge carrier movement, and lowering recombination routes, two-dimensional nanomaterials aid in the hydrogen evolution reaction. They are ideal for surface-related applications because of their strong in-plane chemical bonding and weak van der Waals interactions.

Furthermore, 2D nanomaterials—like nanosheets—offer the benefit of a shorter travel distance for incoming photon flux, which boosts efficiency even under low light conditions. Moreover, the development of p-n nano-heterojunctions on the semiconductor surface highlights the significance of surface chemistry in the construction of heterojunctions, which can improve the hydrogen evolution reaction's overall efficiency. Because of their increased durability against photocorrosion, delayed recombination pathways, and increased efficiency in producing hydrogen, novel heterojunctions made of 2D nanomaterials and their composites have great potential for applications in the future.

The MX_2 heterostructures are intriguing for a variety of applications, especially in the fields of electronics and photovoltaics, due to their numerous noteworthy electronic features. The following are specifics about their electrical characteristics: [47]

A. Band Structure: Direct Band Gaps: Direct band gaps are essential for effective optical absorption and are present in the majority of MXO/MoX_2 heterostructures. When photons are absorbed, direct band gaps enable electrons to go directly from the valence band to the conduction band, increasing the efficiency of devices such as solar cells.
B. Band Gap Quantities: These heterostructures' band gaps are usually between 1.0 and 2.0 electron volts (eV), which is perfect for absorbing most of the sun spectrum. There are few exceptions, though, such as the distorted $HfSeO/MoSe_2$, which may be helpful for applications needing lower energy photon absorption because of its reduced band gap of 0.525 eV.
C. Charge Carrier Mobility: High charge carrier mobility is anticipated in the heterostructures, which is advantageous for applications involving electrical devices. High mobility makes sure that charge carriers can pass through the material rapidly, which lowers energy loss and speeds up the device's reaction time.
D. Interface characteristics and stability: Chemical Stability: Chemical stability is important for long-term device applications, and these materials are typically stable. Device longevity and maintenance needs are impacted by stability. Interface Electronic characteristics: These heterostructures can have distinct electronic characteristics at the interfaces connecting the various layers. These may include band alignment or the creation of interface states, which may have an impact on the material's overall electrical behavior.

E. Versatility in Applications: These heterostructures have a wide range of applications because of their adjustable electronic characteristics. They can be used in sensors, transistors, and other electrical or optoelectronic devices in addition to photovoltaics.
F. Optical capabilities: These materials are appropriate for light-emitting diodes (LEDs) and laser diodes when effective light emission is required since the straight band gaps also indicate significant optical absorption capabilities.

Two-dimensional transition metal dichalcogenides (TMDs) are a newly identified family of 2D materials with properties that make them appealing for applications in nanoelectronics, nanophotonics, and nanosensing. [48]

The TMDs are two-dimensional semiconductor materials with special mechanical, optical, and electrical characteristics. Thus, for the purposes of next-generation semiconductor devices, the materials can make up for the metallic substance graphene and the insulator hexagonal boron nitride (hBN). This section introduces a number of TMD development techniques. While the fundamental principles of manufacturing techniques are transferable to other van der Waals materials, TMDs require a distinct strategy because of their distinct components and growth processes. [49] Although graphene's many fascinating properties have made it very well-known, the search for

two-dimensional semiconducting materials has been fueled by graphene's absence of an electronic band gap, or a material with a zero-band gap.

TMDs have band gap energies between one and two electron volts. [50-53]. TMDs with a monolayer sub nanometer thickness can absorb 5 to 10 percent of incoming light, just like a strong light interaction material.[54-56] These TMD characteristics make the materials suitable for a wide range of uses, including energy harvesting, electrical, optical, sensor, and catalytic applications. [57]

The layered structure of two-dimensional transition chalcogenides (TMDCs), which is composed of two chalcogen planes and a hexagonal transition metal plane, gives TMDCs special electronic transport capabilities. These materials differ greatly from their bulk counterparts in terms of their characteristics, displaying a wide range of electrical flairs and chemical activity. [58]

Molybdenum disulfide

Molybdenum sulphide is a prominent scalable non-precious metal catalyst for hydrogen production, and its use may be essential given the need to lower the cost of these technologies in order to compete with fossil fuels. [59] MoS_2, a two-dimensional sheet of S-Mo-S interlayers placed vertically, has become an unparalleled class of nonprecious HER catalysts with exceptional catalytic activity and outstanding stability in acidic solutions . Due to their excellent potential as a low-cost substitute for the expensive and rare noble metal Pt, as well as the fact that they have hydrogen binding energy comparable to Pt, molybdenum sulfide nanoparticles (NPs) have drawn a lot of attention for hydrogen evolution reaction electrocatalysts (HER). [60]

MoS_2 can be used as a lubricant because of its numerous intriguing features. [61] Although Rapoport, L et.al study will concentrate on MoS_2 as a HER catalyst, 2D transistor and hydro-desulfurization catalyst, [61] Fascinatingly, first research on the electrochemistry of bulk MoS_2 crystals by Tributsch investigations have demonstrated that nanostructuring MoS_2 materials may markedly increase HER activity, reviving interest in this material. [63]

MoS_2 is often found in two polymorphs: 1T-MoS_2, which is the metallic and metastable phase with MoS_6 octahedra, and 2H-MoS_2, which is the thermodynamically stable and semiconductive phase with edge-sharing MoS6 trigonal prisms. 1T-MoS_2 nanosheets exhibit exceptional HER activity in addition to a high electron transport rate.

Compared to other structures, MoS_2 has a higher propensity to create sheet-like nanocrystals due to its distinct layered crystal structure. The impact of MoS_2 phase change on hydrogen evolution performance was initially investigated by Jin and colleagues. They showed that the 1T-MoS_2 was formed directly on graphite and chemically exfoliated from semiconducting 2H-MoS_2 nanostructures by lithium intercalation.[64]

In comparison to lithium (butyllithium-treated) intercalated 1 T MoS_2 nanosheets, the graphite electrode adorned with 2 H MoS_2 nanosheets performed worse in terms of HER. cording to this study, the higher electrical conductivity of the 1 T phase compared to the 2 H phase is what causes the increased HER activity rather than the edge sites becoming stronger. The edge site is catalytically active and may provide an easier path for electrons to hop than the atoms in the basal plane, according to the conventional theory of MoS_2. [65]

When using MoS_2 as an effective HER catalyst, there are often two limitations that need to be taken care of. To enhance the density of the active sites, stacked MoS_2 layers should first be exfoliated. Secondly, the weak electrical connections to the active sites should be strengthened, Therefore, increasing the quantity of these active sites in MoS_2-based electro catalysts is essential to observing a greater activity for HER.[66]

Therefore, because nano-sized MoS_2 has more exposed sulfur edges than the more inert bulk forms, a higher catalytic activity must be seen from it in HER electro catalysis. Although more edge sites can improve the HER activity of MoS2-based electro-catalysts, the function of HER is significantly impacted by this poor inherent electrical conductivity. [67].

Numerous strategies have been put forth to improve the conductivity of MoS_2-based electro-catalysts. MoS_2 is a multilayer transition metal dichalcogenide with strong in-plane bonding within and mild van der Waals forces between the layers. Easy exfoliation into thin layers, which are active for photo-catalytic water splitting, is made possible by this structure. It has been demonstrated that MoS_2's appropriate band gap and effective charge carrier dynamics allow for strong photo-catalytic activity. In conjunction with other photo-catalysts, it can function as a co-catalyst to enhance hydrogen evolution processes.The recombination of photo-generated charge carriers and the comparatively limited absorption of visible light are the key problems with MoS_2. Improving the efficiency of charge separation and visible light absorption are important research areas.
The total HER performance is also influenced by the amount of MoS_2 layers participating in the catalytic process, even though porous shaped electrodes offer controllability over the edge site. [68]

Tungsten disulfide

As a result, hydrogen evolution has received a lot of attention lately. This method has excellent catalytic performance requires adjusted characteristics and a regulated structure. Numerous WS_2 nanostructures were created on this line with the necessary adjustments. WS_2 nanosheets that have been chemically exfoliated under tension are one important method. [69]

A large concentration of strained 1T-phase metallic areas may be seen in the exfoliated WS_2 nanosheets. When WS_2 nanosheets are under tension, they are catalytically active; when they are in compression, they are not. Additionally, strain and variations in the 1 T

phase have an impact on the electrical characteristics of the nanosheets, which is crucial for the nanosheets' catalytic function. Because of this, the as-exfoliated WS_2 with 1 T phase exhibits catalytic activity that is greater than that of the 2 H phase (annealed at 300 ℃) and is similar to Pt nanoparticles. By using an electrochemical method, heteroatom-doped WS_2 yielded MWSx sheets (M 5 Ni, Co). The M-S-W clusters in this system improved the catalytic activity of WS2 nanosheets in hydrogen evolution processes by occupying the MS centers. [70]

Like MoS_2, WS_2 is layered and exhibits weak interlayer van der Waals interactions and high in-plane bonding. This makes it possible to produce thin layers that are advantageous for applications involving photo-catalysis. Photo-catalytic water splitting, especially in hydrogen evolution, has demonstrated the promise of WS_2. It may be adjusted to have a better band gap for absorption of light. Optimizing WS_2's electrical characteristics to improve charge carrier separation and transmission is one of its challenges. Furthermore, much like MoS_2, increasing visible light absorption is still a major challenge. Because of their ability to improve charge separation and decrease recombination, these combinations may result in increased photo-catalytic performance.

Rhenium disulfide

ReX_2 monolayers, which were synthesized lately, are in the family of TMDC semiconductors that do not have a ground-state structure that is either 1H or 1T phase. [71] Layered group VII transition metal dichalcogenides, such as rhenium disulfide and diselenide (ReX_2), have distinct anisotropic optical characteristics that persist from bulk to monolayer. [72] [73]

Y. C. Cheng et al. investigated the structures, and the calculated electronic properties agree quite well with the experimental results. A 2x2x1 super-cell of ReX2 with 48 atoms—16 rhenium and 32 X atoms—was utilized for the doped structures. A 4x4x1 MonkhorstPack 39 grid is used to sample the Brillouin zone for the calculations of total energy. The optical properties, density of states, and electrical band structures were established using a more accurate $8 \times 8 \times 1$ Monkhorst-Pack grid. With a kinetic energy cutoff of 1350 eV, sufficiently converged total energies for the ReX_2 super-cell were calculated.
[74] [75]

According to D. Çakir et al., the Re-d and X-p states make up the bulk of the conduction and valence band edges of ReX_2 structures. The Re-s and X-s states are thus not displayed due to their negligible contributions to the bonding and anti-bonding states. According to prior experimental studies, at the G high symmetry point, ReS_2 and $ReSe_2$ exhibit semiconductivity with a direct band gap (conduction band minimum and valence band maximum are at the same point) of 1.61 eV23 and 1.31 eV20, respectively.

2.2 Photocatalytic Water Splitting

Nowadays, renewable resources account for the majority of hydrogen production. coal, natural gas, and oil[37] While hydrogen has the potential to be a renewable fuel with no emissions, it is currently mostly produced by thermal steam reforming natural gas [76-79]. Although water splitting can produce hydrogen, the high cost of rare earth minerals and precious metal catalysts currently in use makes large-scale application difficult [80-83].

Photocatalytic systems are a crucial tactic for addressing the world's energy need since they enable the production of chemical and electrical energy from sunlight using solar photovoltaics. [84] In order to do this, semiconductor materials with an acceptable band gap must be designed in order to absorb visible light and produce free electrons. [85]

The search for the ideal catalyst for H_2 evolution was started back in 1958. According to Parsons et al., the creation of heat (H_2) on the catalyst surface is directly related to the catalytic development.[85] Furthermore, Norskov and associates developed the capacity to forecast binding energies using computational chemistry, which aided in comprehending the efficiency of H_2 synthesis. [87]

Since 1972, photocatalytic materials have been shown to have the ability to produce hydrogen. [88-90]From then on, a wide range of semiconductor materials have been investigated to assess the extent to which they may produce hydrogen. [91] Finding materials with the ideal band structure is a necessary first step in this search for materials that support charge separation and maintain structural stability over time while also resisting photocorrosion. [92]

Hydrogen (H_2) has a high specific enthalpy and is a clean, carbon-free fuel. Until recently, natural gas accounted for around 95% of the world's supply of hydrogen fuel. Methane and steam are reacted with fossil fuels to generate hydrogen and carbon dioxide (CO_2). Thus, rather than being a form of renewable energy, the process of producing hydrogen from methane is a kind of fossil fuel product. Creating a successful H2-preparation strategy without ever using fossil fuels is a crucial step in using the production of hydrogen. The following reaction equation describes how hydrogen may be produced using photocatalytic materials, and it has been shown since 1972.

$2H_2O \rightarrow 2H_2 + O2$,

$D\mathit{E}0 = 1.23$ eV, $D\mathit{G}0 = +237.2$ kJ mol-1 equ (1)

A thermodynamic "uphill reaction" of solar energy with a significant shift of DG0 = 1.23 eV (237.13 kJ mol-1) per photon powers this photocatalytic activity. According to Equation (2), the photocatalytic materials in this case need four electron generations to withstand this water reaction.

$2H_2O \rightarrow 4H+ + 4e- + O_2$, equ (2)
NHE, pH = 0, *vs*. D*E*0 = 237.13 kJ mol-1

$4H+ + 4e- \rightarrow 2H_2$, equ (3)
NHE, pH = 0, *vs*. D*E*0 = 0 kJ mol-1

In order to create novel architectural materials with superior photocatalytic activity, material scientists make every effort. [93–95]. [96]

The material's morphological dimension is just as important as its chemical composition and structure. When a photocatalytic surface is irradiated with energy more than or equal to its band gap, electron-hole pairs are created. [97] These photogenerated charge carriers produced inside the nanostructure are required to react with the water molecules that are already present on the surface. Along the way to the surface, the charge carriers recombine or get trapped at defect locations. The importance of the energy and time needed by two-dimensional nanomaterials (NMs) for the water splitting process was explained in detail by Ida et al.

Teoh and colleagues identified the bare minimum requirements for a functional photocatalytic system from a critical point of view. [98] These are as follows: (1) the capacity to offer enhanced mobility for charge transfer; (2) the integration of a straightforward synthetic procedure with a productive reaction mechanism; and (3) the significance of photons for demonstrating the nanoarchitectures to access the photoactive sites. [99]

The mechanics of 2D and 3D materials functioning as photocatalysts to split water have been the subject of several published studies. In semiconductors, the absorbed photon must have a greater energy (hn) than the semiconductor's matching band gap in order to excite the electrons from the full valence band (VB) position of the semiconductor photocatalyst to the empty conduction band (CB position). Then, the following formula is used to make the excited pair of electrons and holes (e−− h+):

Photon activation : Semiconductor + hn $\rightarrow$ e− + h+, equ (4)

Oxygen adsorption : (O2)ads + e− $\rightarrow$ O2•−, equ (5)

Water ionization : H2O $\rightarrow$ OH− + H+, equ (6)

Superoxide protonation : O2•− + H+ $\rightarrow$ HOO•. equ (7)

In order to catalyze H_2O into H2 ($H+/H_2$) and oxidize H_2O into O_2 (O_2/H_2O) in a pH = 0 reactant solution at a normal hydrogen electrode (NHE), a single semiconductor photo catalyst's band gap must meet the requirements, as illustrated in Figure 2a, for reduction reaction potential of 0 eV and oxidation reaction potential of +1.23 eV.

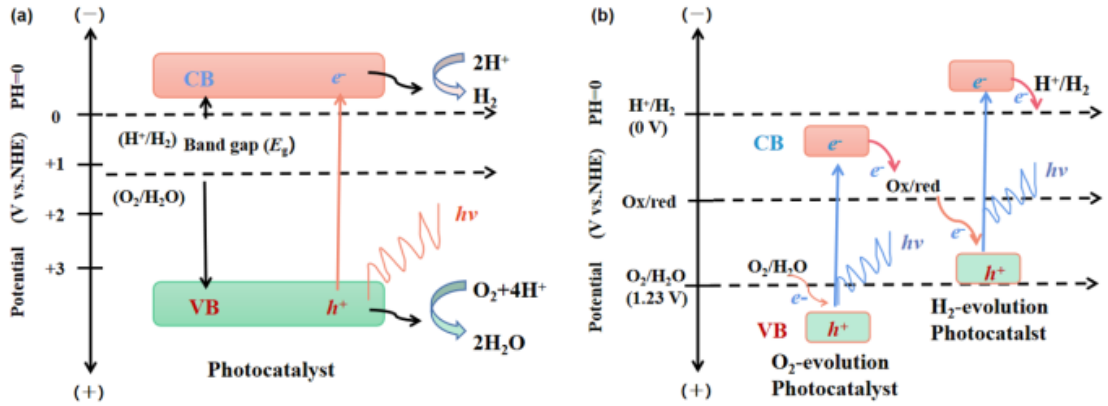

Figure 2. Energy schematic diagram based on (**a**) one-step water splitting (b) Z-scheme system

One-step water splitting is the name given to this process. As an alternative, two or more semiconductors can be connected to a suitable water redox shuttle mediator to create a hybrid semiconductor. In detail, two distinct semiconductors in hybrid materials may undergo H+/H_2 reduction and O_2/H_2O oxidation in order to cause the photon-induced e--h+ couples to break apart and cause general water splitting. We refer to this approach as the Z-scheme system . [100]

Optimizing the HER's rate requires the employment of a catalyst with the proper surface properties. Numerous material groups, such as nickel alloys, metal oxides, metal phosphides, metal sulfides, and precious metals like platinum, have been investigated as active HER catalysts.

Even though transition metal dichalcogenides have lately drawn interest as a potentially useful class of materials for electro catalysis, precious metals still outperform them in terms of durability and activity.

The utilization of photocatalytic water splitting in solar-to-hydrogen conversion is a viable approach for achieving sustainable hydrogen generation. Highly active, reasonably priced, and naturally occurring materials are needed as photocatalysts in the photocatalytic process. Molybdenum disulfide (MoS_2) is a presentative layer-structured transition metal dichalcogenide that is gaining a lot of attention because of its special electro and optical characteristics.

The only source of energy that can provide enough energy is the sun [101]. However, solar energy is intermittent and needs to be stored effectively . One of the more appealing techniques for storing solar energy is the splitting of water driven by sunlight to create hydrogen. [102]

2.3 Photovoltaic Solar Cells

Although graphene has been used for several purposes in solar systems, its low absorption coefficient and metallic behavior due to the lack of a band gap make it difficult to utilize as the absorber layer. As Ultrathin 2D TMDs are more abundant and have more varied electrical characteristics than graphene, which makes them appealing for a range of solar cell device applications. [103] Recent developments in ultrathin two-dimensional nanomaterials have led Chaoliang Tan et al. to study 2D TMDs as counter electrodes in DSSCs and QDSCs, as well as as charge transport layers in organic solar cells and light absorber layers. [104]

It has been anticipated that a 0.9 nm thick MoS2/graphene bilayer solar cell might attain a PCE of up to 1%. While the efficiency is extremely low, the power density (up to 2.5 MW/kg) is around 1-3 orders of magnitude greater than the conventional GaAs and Si solar cells with larger active layers (>1 μm). Shanmugam et al. discovered that the graphene thickness affected the photovoltaic performance of this solar cell.

In Shanmugam's study, light-absorbing layers were successfully added to glass substrates coated with ITO using CVD-grown MoS2 and WS2 nanosheets. Following the deposition of top metal contacts with suitable work functions, a Schottky barrier junction is produced. The PCE of solar cell devices using the ITO/MoS2/Au and ITO/WS2/Au combinations was 1.8% and 1.7%, respectively.

Different from graphene, the intrinsic semiconducting behaviors of some TMDs make them possible to be used as photoactive layers in solar cell devices. Theoretical calculations indicate that 2D TMDs can absorb up to 5-10% of incident sunlight in a thickness of less than 1 nm, which is comparable to the light absorption property of 50 nm-thick Si.The excellent absorption properties of monolayer TMDs are highly desirable to fabricate ultrathin photovoltaic devices by using 2D TMDs as building blocks. To be a prerequisite, ultrafast charge transfer was observed in the atomically thin MoS2/WS2 heterostructure, and photovoltaic power generation was demonstrated in the monolayer WSe2-based p-n junction, although the conversion efficiency is low. [105]

2.4 Previous Research on heterostructures

Similar two-dimensional (2D) sheet-like designs have been demonstrated for semiconductors with significant active surface area and electrical mobility in comparison to their bulk form since the discovery of graphene. [106]. Transition metal dichalcogenides (TMDs) in two-dimensional nanomaterials are receiving a lot of interest in this context. The standard chemical formula for TMDs, which are atomically thin semiconductors, is MX_2 (where M is an atom of a transition metal, like Mo, W, Ta, or Nb, and X is an atom of a chalcogen, like S, Se, or Te). The MX bond is covalent, and this is referred to as MX_2 in a single unit. Multiple TMD layers stacked on top of one

another provide a bulk TMD material in cross section, with weak Van der Waals (vdW) forces holding the layers together. For the first time, it was shown by Nørskov and colleagues that the MoS_2 edge's ΔGH value is thermoneutral and serves as the active site for the hydrogen evolution process (HER). [107]

The 2D heterostructure known as transition metal dichalcogenides (TMDs) has special structural and physical properties. With their multilayer structure, visible-wavelength band gaps, high carrier mobility, high on/off current ratio, and valley-spintronic characteristics, these heterostructures are appropriate for a range of electrical and spintronic applications. TMDs are categorized according to their structural arrangements and chemical makeup as insulators, semiconductors, semimetals, and superconductors. [108]

The electrical and optical characteristics of layered MX_2 (TMDs) are encouraging, increasing their potential for use in optoelectronic and electronic applications. These characteristics make transition metal dichalcogenide-based 2D heterostructures an attractive platform for investigating fundamental physics and creating advanced electrical and optoelectronic devices. Monolayers of TMDCs, such as WS_2 and MoS_2, have direct semiconducting band gaps in the visible spectrum, contrasting with their bulk phase's indirect band gaps. [109]

This important investigation has led to substantial advancements in 2D TMDs research focused on increasing the density of active edge sites and has provided critical proof that the MoS_2 active sites are localized at the edge planes. This research was followed by an investigation by Jaramillo et al. [110] on how MoS_2 structures imitate their active sites in a manner similar to that of natural catalysts like the enzymes hydrogenase and nitrogenase. This work also shown a linear link between the edge length of MoS_2 and its electrochemical HER activity.

TMDs may be found in a variety of polymorphs of 2 H, 1 T, and 3 R in the matching rhombohedral, trigonal, and hexagonal forms. In contrast, the 2 H and 3 R phases are semiconducting. By restacking, the resultant monolayer 1T-MoS_2 tends to create more stable 2H-MoS_2, which is thermodynamically metastable. As a result, a multiphase of the 2 H type typically contains the 1 T phase. TMDs that are often seen crystallize in the 2 H or 1 T phases, where the chalcogen atom and transition metal have trigonal, prismatic, or octahedral bonding arrangements. The transition metal's nonbonding d orbitals in 2H-phase TMDs break into three degenerate states: dxz, yz (e0), d2 x 2 y2, and d2 z (a1). In contrast, degenerate d2.z; x2; 2; y2 (eg); and dxz,yz,xy (t2g) orbitals are formed by 1T-phase TMDs. [111]

Similar to graphite, 2D TMDs are made up of monolayers that are joined by Van der Waals attraction. Because of their ultrathin structure (~0.6–0.7 nm) and high surface-area-to-mass ratio, 2D TMDs are ideal for loading a wide range of biomolecules. In bulk TMDs, the gap is indirect, but in the monolayer state, it is direct. Transistors may be

made from MoSe, MoS, WSe, WS, and MoTe monolayers as they have direct band gaps and electron mobilities that are similar to silicon's. The electrical structure of semiconducting TMDs, such as WS, WSe, and MoS, shifts from an indirect to a direct band gap when they are thinned to a single layer. The emerging technologies in the electrical and optoelectronic domains have garnered attention following the finding of a direct band gap. TMDs may be manipulated to create materials with various magnetic characteristics, such as ferromagnets, antiferromagnets, or paramagnets, as well as semiconductors, metals, or superconductors. [112]
Due to their superior charge/discharge capabilities, stability, extended life, and very high surface Li diffusivities, TMD-based (MX2) electrodes have emerged as viable alternatives.[113] [114] According to a study by Jiang et al., the best heterostructure for Li atom storage is one composed of alternating graphene and MoS2, as this combination not only increases MoS_2's electrical conductivity (particularly in the c-direction) but also prevents aggregation and promotes the restacking of MoS2 nanosheets. [115]

P. Liu et al. discuss about the synthesis, characteristics, and uses of 2D heterostructures made of transition metal dichalcogenides. Their distinct structural and physical characteristics are highlighted, along with their possible uses in valley-spintronics and nano-optoelectronics. Their focus lies in creating atomically thin heterostructures with distinct layers of MX_2, which offer a fresh avenue for investigating fundamental physics and developing novel devices.[116]

Interesting and novel physicochemical features for vertical and in-plane G6-TMD heterostructures are predicted by first-principles computations. Currently a hot research issue, heterostructuring has opened up a new path in the realm of 2D materials for creating artificial materials with specific optical and electrical characteristics. Different heterostructures are used in the case of G6-TMDs, such as in-plane MoS_2-WS_2, vertical MoS_2/WS_2, MoS_2/WSe_2, WS_2/MoS_2, MoS_2/grapheme and MoS_2/hBN heterostructures. Heterostructures MoS_2–$MoSe_2$, WSe_2–MoS and $MoSe_2$–WSe_2 have all been synthesized. [117]

The discussion was then expanded by Cavallo's group to include materials at the MoS_2-WSe_2 monolayer's interfacial area that had comparatively few defects. They replicated the measured band gaps of WSe_2 and MoS_2 monolayers to verify their calculations. [118]

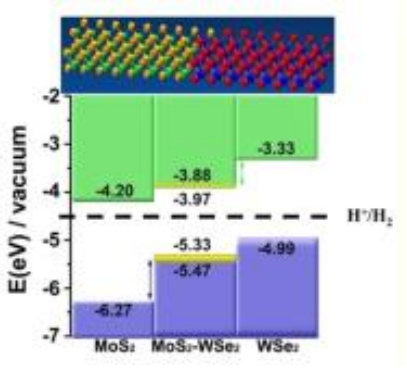

Figure 3. VBM and CBM energy alignment of the pure MoS_2 and WSe_2 monolayers as well as for their LHJs with representative types of defects using vacuum as a reference. The range of the calculated MoS_2-WSe_2 band gaps is indicated. Reprinted with permission from ref 118. Copyright 2017, American Chemical Society.

The higher CBM energy level of the WSe_2 monolayer compared to the MoS_2 monolayer led to a type II heterojunction. The CBM energy levels of the projected LHJs were found to be between the pure MoS_2 and WSe_2 monolayers. The CBM energy levels for sharp and faulty heterojunctions varied somewhat (0.1–0.2 eV), but this difference did not substantially alter the overall pattern with CBM offsets in the 0.55-0.64 eV range.

The energy band alignments of the pure monolayers before and after contact indicate that the MoS_2-WSe_2 LHJ is a prominent p-n junction, as reported in previous studies. Although both MoS_2 and WSe_2 monolayers showed suitable CBM energy levels for HER with relative values of 0.3 and 1.17 eV higher than the $H+/H_2$ potential, respectively, LHJs also showed appropriate CBM energy positions within a 0.53–0.62 eV range higher than the H+/H2 potential, highlighting another class of suitable materials for HER. [119]

Chapter 3: Computational Methodoogies

3.1 Density Functional Theory (DFT)

Density functional theory (DFT) is one of the most widely used and adaptable techniques in the study of solid-state inorganic materials for determining the energies and structural composition. An approximate, accurate, and cost-effective solution to a Schrödinger equation may be found via DFT. The electronic charge density is a homogeneous quantity that is linked to all of the interactions according to density-functional theory (DFT). [120] The early developments of modern DFT were greatly aided by the Hohenberg-Kohn theorems[121] and the work of Kohn and Sham[122].

Quantum ESPERESSO and CASTEP were utilized to investigate 2D hexagonal transition metal dichalcogenide heterostructures as potential materials for hydrogen evolution processes using density functional theory. The Generalized Gradient Approximation (GGA) with the Perdew-Burke-Ernzerhof (PBE) functional and the local density approximation (LDA) for the studied triclinic transition metal dichalcogenide were used to explain the exchange correlation functional. The Quantum ESPRESSO and CASTEP module implemented spin polarized density functional theory with van der Waals (vdW) computation. [123]

The Perdew-Burke-Ernzerhof (PBE) approach was used to correct the exchange-correlation (XC) functional, norm-conserving pseudopotential and the van der Waals (vdW) semi-empirical dispersion correction, as implemented in the Quantem ESPRESSO.

[124] [125]

HOHENBERG-KOHN THEOREMS

By employing the electronic density as a critical parameter rather than the wave function, the Hohenberg-Kohn theorems, which are the cornerstone of density functional theory, provide a fundamental framework for resolving complex many-body problems [126]. The Born-Oppenheimer equation is challenging to solve because the electrons and nuclei that comprise materials constitute a strongly interacting many-body system that is currently unsolvable. Density functional theory may be used to get an approximation to the ground state of a many-body system.

"The ground state of any interacting many particle system with a given fixed inter-particle interaction is a unique functional of the electron density n(r)," according to the first Hohenberg–Kohn theorem. (Kohn and Hochenberg, 1964). This suggests that the ground state wave function may be expressed as a unique functional of the ground state electron density, i.e., $\psi 0 = \psi[no]$, by inverting Eq. (). As seen in Eq. (8), this will allow one to express the ground state energy E as a functional of the ground state density.

$E[\psi[n_o]] = \{\psi[n_o] | \check{T} + \acute{o} + \check{U} | \psi[n_o]\}$ equ 8

This feature, together with a related variational theorem, has led to the development of useful empirical representations of the density functional, which enable accurate electronic energy estimate even in complex chemical systems. Previously, it was thought that these functionals depended only on the local density. The empirical functionals were thought to rely on the kinetic energy density, the occupied orbitals, the gradient of the densities (in the generalized gradient approximation, or GGA), and ultimately the unoccupied orbitals over time.
[126]

KOHN-SHAM EQUATIONS

According to Kohn and Sham's theorem, an analogous non-interacting electron system with the same external potential has a ground state density that is identical to the original interacting system's. First, a set of hypothetical non-interacting electrons is used to solve the Kohn-Sham equations. The way these electrons are used guarantees that their density is precisely the same as the density of the actual system.

The Hohenberg-Kohn theorem's functional may be helpfully expressed in terms of the single-electron wave function, $\psi i [n(r)]$. The functional given in Equation (9) may now be expressed as

$E[\psi_i[n(r)]] = E_{known}[n(r)] + E_{xc}[n(r)]$ equ 9

DFT utilizes a combination of the Hohen berg-Kohn theorems and the Kohn-Sham equation to solve the Schrödinger equation for a given system.

EXCHANGE-CORRELATION FUNCTIONAL

Due to the enormous amount of processing power needed to achieve a precise value of the correlation energy, correlation in particular has historically proven to be challenging to compute. The exchange and correlation potentials, however, are solely functional of the local density in the Kohn-Sham equations. Because of this, calculating these energy is manageable. Finding an accurate approximation of this amount is essential to the correctness of the entire DFT approach. The LDA or GGA, which may be considered an extension of the LDA, are now used to create most functional approximations for the exchange-correlation functional.

3.2 Computational Tools

Quantum ESPRESSO is an integrated suite of open-source computer codes for electronic-structure calculations and materials modeling at the nanoscale. It is based on the density-functional theory (DFT), plane waves, and pseudopotentials. It is one of the Materials Studio offers DFT codes for conducting material simulations. The Quantum Espresso package is a distribution of related programs that can be expanded. Two main tools for DFT electronic structure calculations, PWscf (Plane Wave self-consistent field), and CP (Car-Parrinello Molecular Dynamics) are complemented by numerous packages for particular applications as well as plug-ins. for a given system is a science in itself.

Functions like the electron density or wave function must be expanded in a basis set in order for a computer to simulate materials. According to Bloch's theorem, plane waves serve as the basis for Quantum Espresso. It is a Fourier series expansion of functions for the Gamma point. An energy cutoff (ecutwfc, ecutrho) can be used to achieve a finite number of expansion coefficients, which are necessary for computing. Without significantly altering the outcome, pseudo potentials are employed to smooth the Coulomb potential by atomic nuclei, resulting in fewer plane waves. Several pseudo potentials (PAW, ultrasoft, and norm-conserving) can be used with Quantum Espresso. Selecting a system's pseudo potential is a science unto itself.

Materials Studio is a comprehensive software suite developed by BIOVIA, used for materials modeling and simulation. It is widely used in computational materials science and chemistry for modeling, simulating, and visualizing the properties and behavior of materials at the atomic and molecular level. It is used by researchers, scientists, and engineers to develop new materials, optimize existing ones, and gain insights into the fundamental properties of various substances. Material Studio implements quantum mechanical methods, such as Density Functional Theory and Hartree-Fork, to calculate electronic structures, optical properties and other quantum level characteristics.

Materials Studio provides a range of tools to build and visualize complex hetero-structure models, allowing for precise control over atomic arrangement and layer composition. It also analyzes the interface between different layers in the hetero structure. Constructing a super cell in Material Studio involves creating an enlarged periodic structure based on a unit cell. Adjusting lattice mismatch in Material Studio typically involves modifying the lattice parameters of one or more materials to create a compatible interface, which is necessary when studying hetero structures. Creating a super cell can help match the lattice parameters more effectively by adjusting the replication factors to make the lattice parameters of the materials more compatible. After the lattice parameter adjusted the supper cell will build by aligning the materials appropriately and combine them in to a single model.

First-principles calculations were carried out on the monolayer of MoS_2, WS_2, ReS_2 and for hetero-structures MoS_2-WS_2, ReS_2-WS_2 and ReS_2-MoS_2 using DFT with a plane-wave basis along with Projector Augmented Wave (PAW) pseudo potentials (PP)[127].

These calculations were performed through the implementation of Quantum-ESPRESSO and CASTEP codes [128][129]. The geometry optimization calculations were performed using the GGA-PBE method, which incorporates a van der Waals correction through the gramme-D2 method [130].

All DFT calculations of the monolayers MoS_2, WS_2, ReS_2 and for heterostructures MoS_2-WS_2, ReS_2-WS_2 and ReS_2-MoS_2 have been performed using PBE ultrasoft pseudo-potentials for core interaction under the framework of Quantum-ESPRESSO. In this work first, we decide the appropriate values of the K-point, cutoff energy (wfc), charge density (ecutrho), and lattice parameter. Self-consistent calculations (convergence test) were performed by adjusting the system card parameters to obtain a converged minimum total energy. For geometric optimization, the 'relax' calculation is performed to optimize the atomic position of the monolayer and heterostructure. The geometric Structures are relaxed until forces are below 1 meVÅ^{-1}.

The most stable hetero-structures employing 2D semiconductors require minimum lattice mismatch (usually less than 5%). Heterostructures are essential for the formation of vdWHs because of their well-suited structural character. Multilayer vdWH, in which individual covalently linked layers are held together by weekly vdWH forces without dangling bonds, is a promising method of merging several 2D materials to attain desirable features for many TMDs. By aiming to harness the above-mentioned properties of the heterostructure we have constructed heterostructures such as ReS_2-WS_2

The lattice mismatch calculation was performed using the formula: A to B equ 10

$$\text{Lattice mismatch (\%)} = \frac{\text{Lattice parameter (A) - Lattice parameter (B) x 100}}{\text{Lattice parameter (A)}}$$

A super cell (SC) is an artificial mathematical construction obtained by stacking a primitive cell (PC) along one or more spatial directions. The PC building block of the SC has to be understood only as lattice (basis vectors and atomic positions) and not as crystal structure (lattice vectors and atomic basis). In this context, the SC has long been used in those electronic structure calculation methods that rely on periodic boundary conditions. [131-133] Since the concept of the SC in terms of site occupancy is arbitrary, this method affords a flexible description of absence of order.

One can usually see the SC as a stacking along all or some of the three spatial directions of the PC of a Bravais lattice. The PC lattice vectors āi (i = 1,2,3) make up the building unit for the SC vectors Āi. Here and in the following we denote by small (capital) symbols quantities referring to the PC (SC). In matrix notation, the two sets of basis vectors are related by Ā= M · ā, or [134]

$$\begin{pmatrix} \bar{A}1 \\ \bar{A}2 \\ \bar{A}3 \end{pmatrix} = \begin{pmatrix} \mathrm{m}11 & m12 & m13 \\ m21 & m22 & m23 \\ m31 & m32 & m33 \end{pmatrix} . \begin{pmatrix} \bar{a}1 \\ \bar{a}2 \\ \bar{a}3 \end{pmatrix}, \text{ mij } \varepsilon\, \mathbb{Z}\,, \qquad \text{equ 11}$$

where the only condition imposed on the transformation matrix M is to be invertible (nonsingular). In the most general case, M does not need to be diagonal, that is, the SC and PC unit vectors do not need to be collinear. The elements of M are integers ($mij \in Z$), which corresponds to the case of a SC commensurate [135] to the PC, the only one considered here.

Chapter 4: Result and Discussion

4.1 Construction of Hetero-structures

4.1.1 Convergence Test for Monolayer TMDs

Convergence testing is a technique for improving simulations to use computational resources efficiently and produce useful findings. It is a mathematical technique used to determine whether a sequence or series approaches a specific value as it progresses or if it is diverges, meaning it does not approach any meaningful limit. It helps us to determine whether a series number is reaching a stable and well-defined result or if it is fluctuating or heading towards infinity. In this study, we performed various SCF calculations for the k-points grid, kinetic energy cutoff, charge density cutoff, and lattice parameter optimization to determine the fundamental parameters to obtain the optimum energy.

Table 1 : converged value of monolayer MoS_2, WS_2 and ReS_2

	Monolayer		
	MoS_2	WS_2	ReS_2
k-point	12x12x1	12x12x1	13x13x1
Cutoff energy	90Ry	120 Ry	120 Ry
Ecutrho	270 Ry	1080Ry	1080 Ry

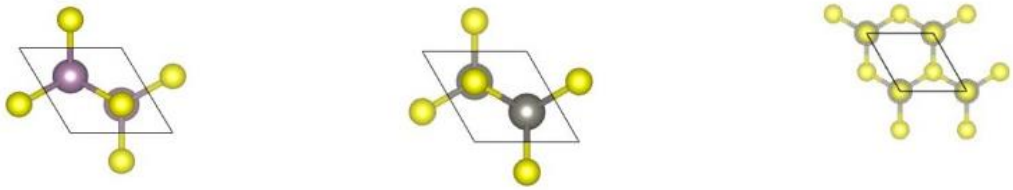

MoS_2 **WS_2** **ReS_2**

Figure 4 Converged value of monolayer MoS_2, WS_2 and ReS

The K-Point Optimization

In order to do calculations for real-space unit cells with a large number of atoms, early computational efforts concentrated on an inexpensive choice of k-points for Brillouin zone sampling [135]. However, a better collection of specific k-points should be employed for accurate calculations. To get more precise findings, more grid points can be acquired, but this comes at a high computational cost. Total energy was calculated using SCF utilizing a variety of k-point grids, from 1×1×1 to 16×16×1. As seen in Figure 5, the total energy fluctuates based on the shift in k-points and converges.

We could start with the values of 7x7x1 to determine the appropriate basis set size because the total energy and k mesh values converged linearly from that point on. For MoS_2, WS_2, and ReS_2 monolayers, the ideal set of k-point values was chosen with a notably modest total energy change, taking into consideration the constraints of computational resources.

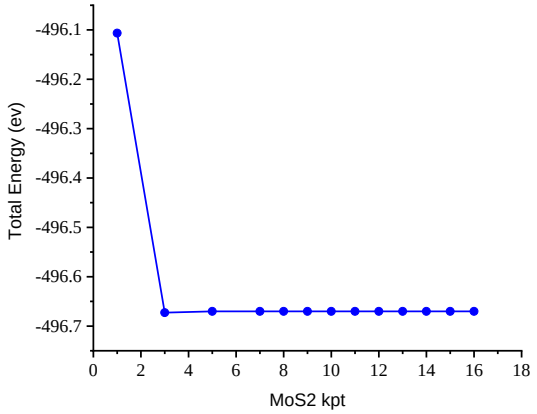

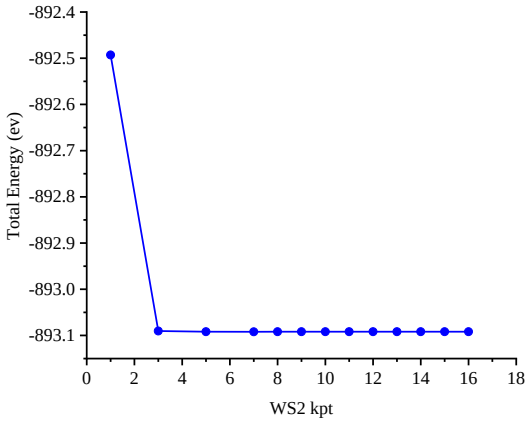

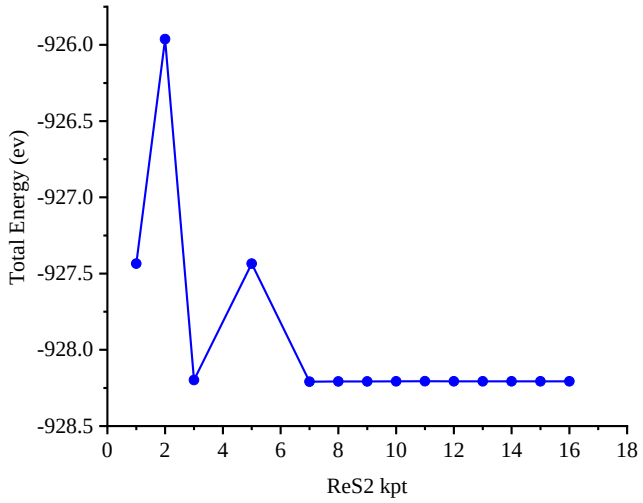

Figure 5: Energy Vs. K-point of (a) MoS_2 and (b) WS_2 (c) ReS_2 monolayers computed using PBE

Basis Set Size

The two important cutoff energy-related flags, Ecut (wfc) and Ecut (rho), can be found in the SYSTEM card name list if the Quantum ESPRESSO module's scripting is general. Ecut (Wfc) indicates cutoffs for wave function kinetic energy, while Ecut (rho) indicates cutoffs for charge density. The number of plane waves that Ecut specifies can be used to compute the DFT. The number of plane waves must be changed to strike the right balance between the maximum kinetic energy cutoff and the number of plane waves. It is crucial to maintain Ecut(rho) as a multiple factor of Ecut(wfc) during computation.

First, we can modify it while keeping Ecut(rho) at the same factor time as Ecut (wfc). Once the proper value for Ecut (wfc) has been determined, the same situation may be replayed for Ecutrho.

According to the figure, convergence is attained with increasing total energy and Ecut (Wfc).

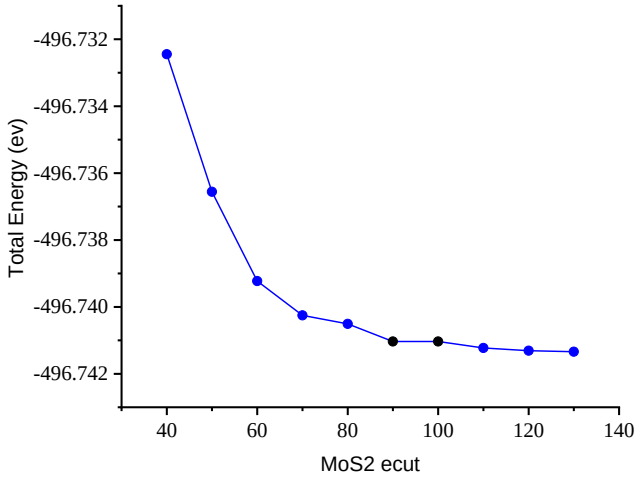
-496.732
-496.734
-496.736
-496.738
-496.740
-496.742
Total Energy (ev)
40
60
80
100
120
140
MoS2 ecut

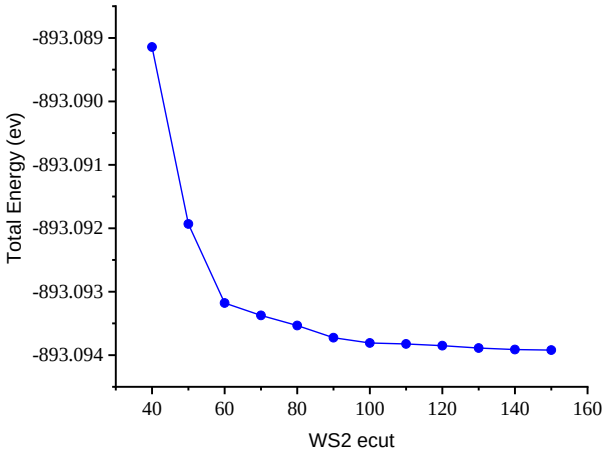
-893.089
-893.090
-893.091
-893.092
-893.093
-893.094
Total Energy (ev)
40
60
80
100
120
140
160
WS2 ecut

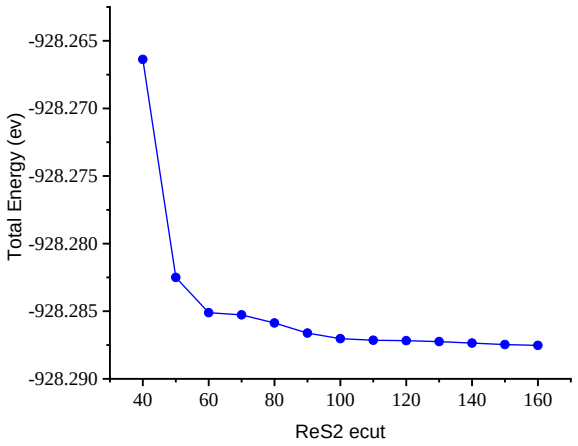
-928.265
-928.270
-928.275
-928.280
-928.285
-928.290
Total Energy (ev)
40
60
80
100
120
140
160
ReS2 ecut

Figure 6 :Total Energy Vs. Ecut of (a) MoS_2 and (b) WS_2 (c) ReS_2 monolayers computed using PBE

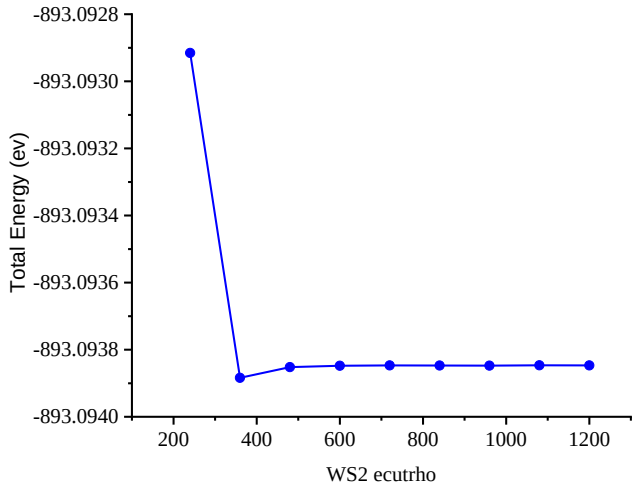

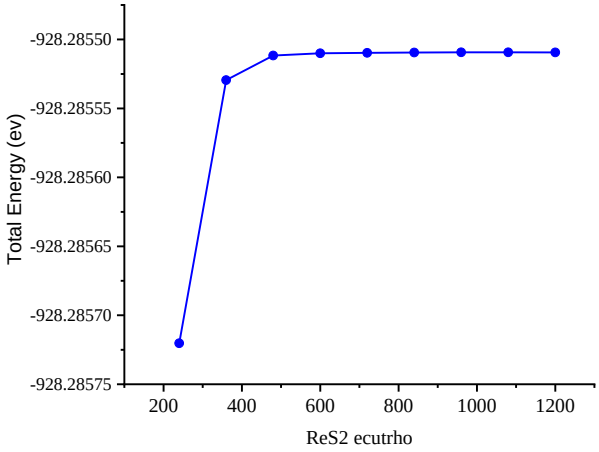

Figure 7: Total Energy vs. Ecutrho of (a) WS_2 (b) ReS_2 monolayers computed using PBE

Lattice Constant Optimization

Following optimization of the crystal lattice constant of monolayers, 2D heterostructures of MoS_2-WS_2, ReS_2-WS_2, and ReS_2-MoS_2 have been built. Consequently, monolayers of MoS_2, WS_2, and ReS_2 are crucial for designing TMD heterostructures. By offering a lattice constant that, when lattice constant optimization is performed, yields the least amount of energy beyond the expected value when computing the total energy of MoS_2, WS_2, and ReS_2.

Following each round of the computations, we obtained new total energy and lattice constants. Until we got the lowest overall energy, the iteration went on. To provide a stable atomic location for the subsequent computation, the crystal structure must be relaxed after gating the minimal total energy and optimizing the lattice constant.

Figures (a, b, and c) show the optimized/calculated lattice parameters of the MoS_2, WS_2, and ReS_2 monolayers in the ranges of 3.192 Å, 3.184 Å, and 2.917 Å, respectively. As a result, this figure represents the lowest monolayer total energy. The optimized lattice parameters of MoS_2, WS_2, and ReS_2 are shown in the table along with comparisons to those of prior investigations.

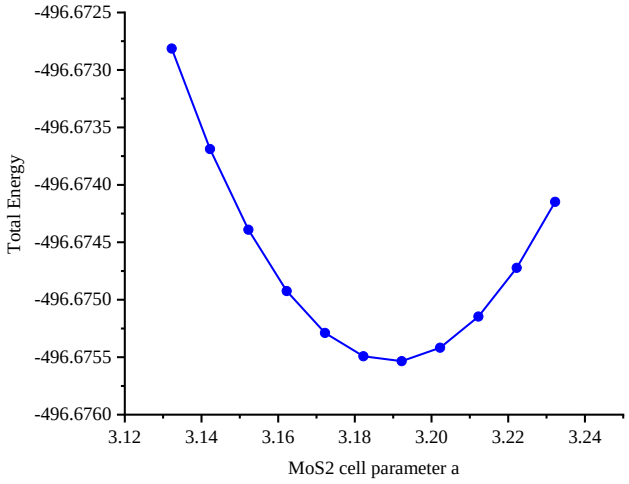

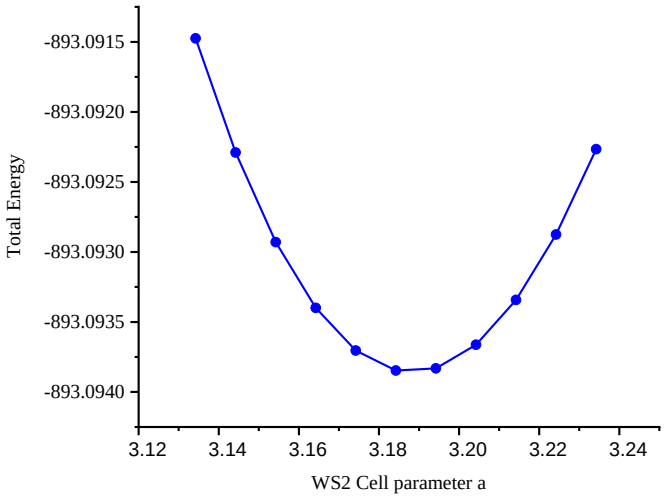

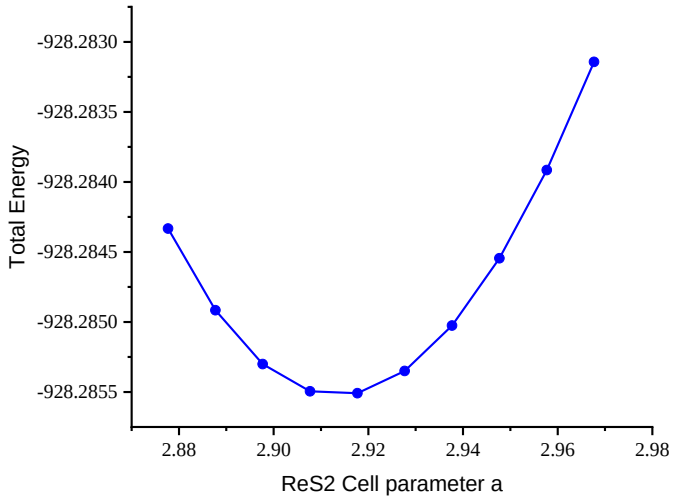

Figure 8: Total energy Vs. lattice parameter of the (a) MoS_2, (b) WS_2 and (c) ReS_2 monolayers computed using PBE

4.1.2 Using Materials Studio

The synthesis of heterostructures, including tungsten disulfide (WS_2), molybdenum disulfide (MoS_2), and rhenium disulfide (ReS_2), is a crucial technique in the development of 2D semiconductor-based water splitting photo catalysts. These heterostructures enhance light absorption, charge separation, and catalytic activity by utilizing the unique properties of each material. The heterostructures have several key features, including enhanced light absorption due to the broadened absorption spectrum, better charge separation and transfer through Type-II hetero-junctions, and synergistic effects due to increased catalytic sites, electrical conductivity, and mechanical stability. They also offer multiple active sites for catalysis processes, such as oxygen evolution reaction (OER) and hydrogen evolution reaction (HER). [136]

Moreover, the combination of these substances improves the photo catalyst's stability compared to their constituent parts. Research in photo catalysis combines theoretical models with experimental synthesis and characterization to anticipate and optimize the features of these heterostructures. This approach enhances the efficiency of photocatalytic devices and helps understand the underlying processes at work. The development of heterostructures combining MoS_2, WS_2, and ReS_2 is an interesting topic in photocatalysis, as it allows for enhancements in light absorption, charge dynamics, and catalytic activity, which are essential for effective solar-driven water splitting.

Table 2 : Lattice Parameters and Lattice Mismatches of Monolayers Calculated

MX_2	lattice constant **a(Å)**	Calculated mismatch value (%)
MoS_2	3.192	
WS_2	3.184	
ReS_2	2.917	
MoS_2 Vs WS_2		0.25
ReS_2 Vs WS_2		8.37
ReS_2 Vs MoS_2		8.6

Table (2) demonstrates that the MoS_2 and WS_2 layers are fully coherent and that the lattice misfit of the optimized lattice parameters of the two monolayers is less than 5%. Because of the tiny MoS_2/WS_2 lattice mismatch (0.25%), hetero-structures may be designed with respect to vdW interactions, and experimental fabrication of the structures is possible. Using MoS_2 and WS_2 monolayers, novel 2D hetero-structures were created based on first-principles calculations.

The two monolayers, MoS_2-ReS_2 and ReS_2-WS_2, have optimal lattice parameters with lattice mismatches of above 5%, whereas MoS_2/ReS_2 and WS_2/ReS_2 had lattice mismatches of 8.6% and 8.37%, respectively.
Therefore, it requires to build optimized super cells and construct the heterostructure using the super cells to make the lattice mismatch less than 5%.

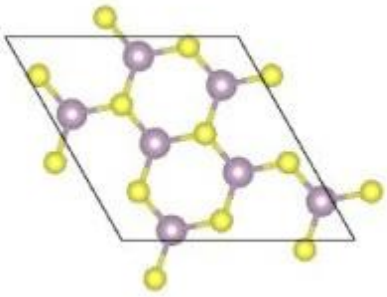

MoS_2 super-cell

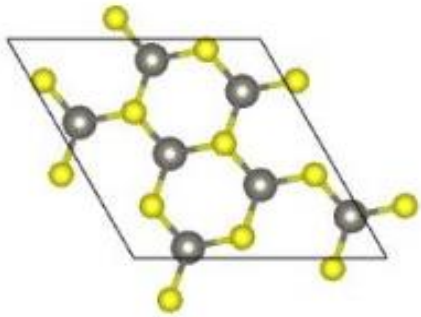

WS_2 super-cell

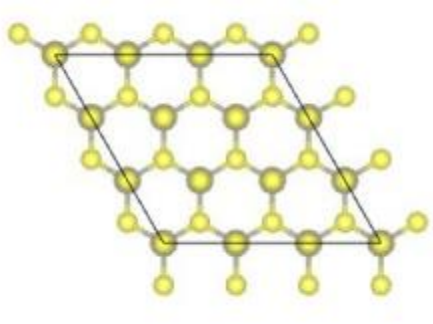

ReS_2 super-cell

Figure 9 : Super cell of MoS_2 , WS_2 & ReS_2

After constructing the supercells, we found out that, the lattice parameter for super cell MoS_2, WS_2 and ReS_2 is 8.44587 **Å**, 8.42466 **Å** and 8.75309 Å and the lattice mismatch of super cell ReS_2 with WS_2 and ReS_2 with MoS_2 are below 5%. So for the rest of this research we can use those super cell for the formation of hetero structure.

Table 3 : Lattice Parameters and Lattice Mismatches of Super Cell Calculated

Supper cell	lattice constant **a(Å)**	Calculated mismatch value (%)
MoS_2	8.44587	
WS_2	8.42466	
ReS_2	8.75309	
MoS_2 Vs WS_2		0.25
ReS_2 Vs WS_2		3.7
ReS_2 Vs MoS_2		3.5

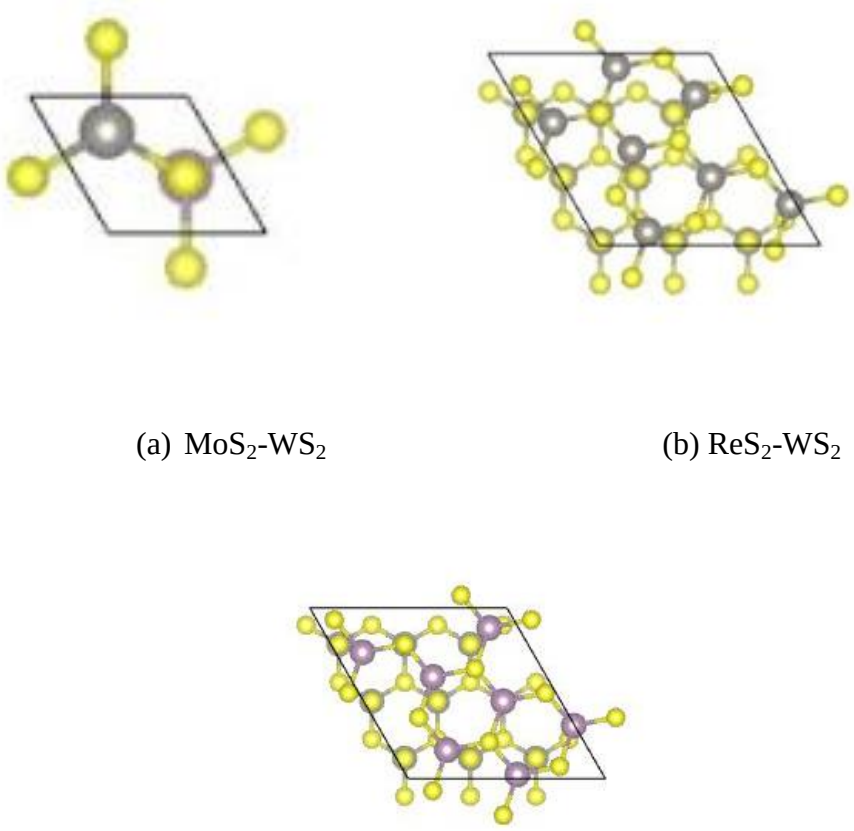

(a) MoS_2-WS_2 (b) ReS_2-WS_2

(c) ReS_2-MoS_2

Figure 10: (a) Hetero structure formed from monolayer MoS_2 and $WS_2$and (b)and (c) heterostructure formed from super cell MoS_2, WS_2 and ReS_2

4.1.3 Structural Optimization

Structural optimization in DFT calculation is finding the structure that minimizes the total energy of the crystal. Indeed, you could make a few calculations with different values for this z-coordinate, and search for the value that minimizes the energy. More complex crystals will easily have 5, 10 or more such degrees of freedom, which will make such an explicit calculation procedure rapidly too expensive. There are two types of structural optimization in QE,(1)relax: where only the atomic positions are allowed to vary, and (2) vc-relax: which allows to vary both the atomic position and lattice constants.

When the materials are ready to search for the optimal values of a , b and c lattice parameters. One way to do this, is to do DFT calculations for all possible values of a b and c, and find out which value gives the lowest total energy (ideally, for every single

choice of a, b and c, the z-value has to be optimized too) . An alternative (and faster) way is to use an automatic optimization procedure within QE that searches for the set of lattice parameters, unit cell angles and internal positions that makes the stress tensor zero (which corresponds automatically to a minimal total energy).[137]

The "relax" computation is used for geometric optimization in order to maximize the atomic positions of the hetero-structure MoS_2-WS_2, ReS_2-WS_2, and ReS_2-MoS_2 as well as the monolayer MoS_2, WS_2, and ReS_2. We relax the geometric structures until the forces are less than 1 meVÅ-1.

4.2 Electronic Properties

4.2.1 Band Structure

Band structure of monolayer TDMs

Transition metal dichalcogenides (TMDs) are composed of three layers; top and bottom layers of chalcogen atoms and middle layer of transition metal atoms. The bandgap of TMDs (WS_2, MoS_2, WSe_2, and $MoSe_2$) changes from indirect to direct bandgap when the materials are thinning from bulk to monolayer [138]

Figure 11 show the band structure plot from this specific research of hexagonal monolayer TMDs of MoS_2, WS_2 and ReS_2. The band gap energy of MoS_2 is 1.6804 ev with the higher occupied level of -2.0449 ev and lower unoccupied level of -0.3645ev.

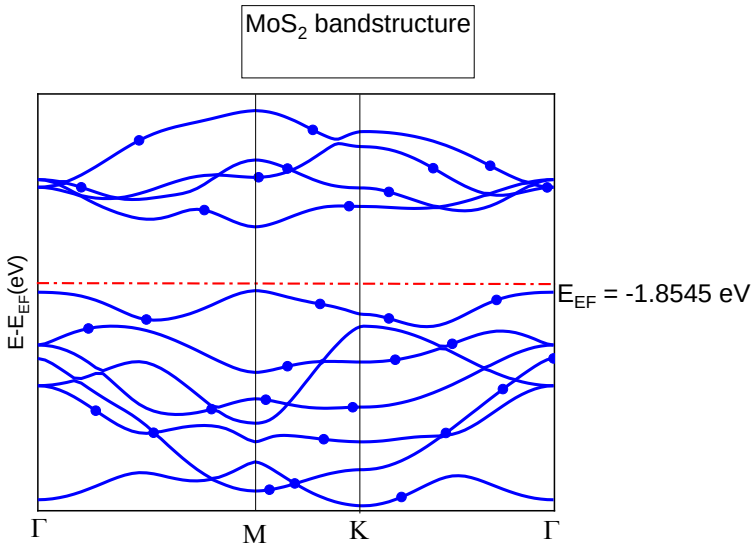

(a)

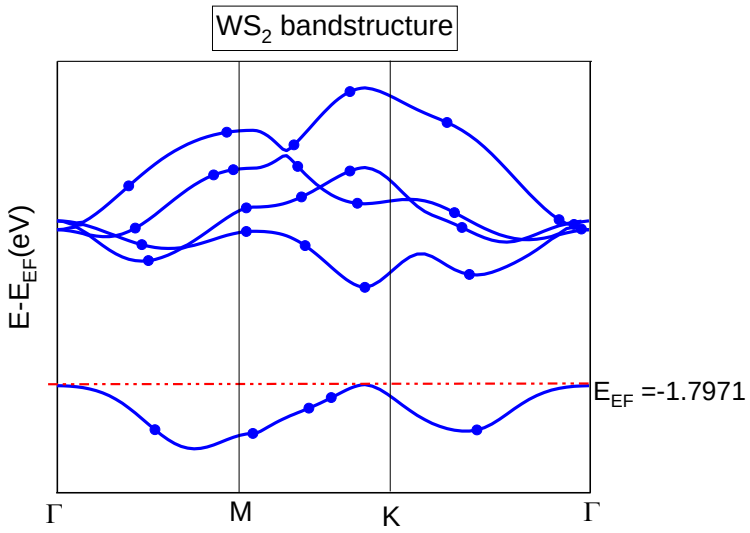

(b)

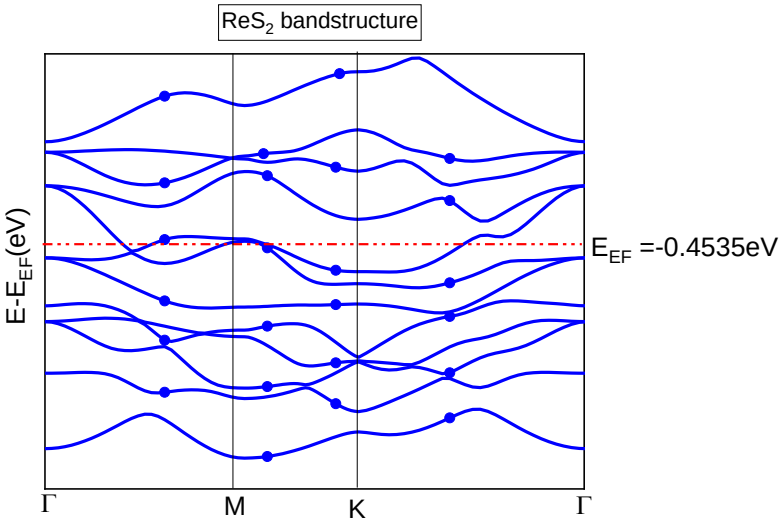

(c)

Figure 11: Band-structure (a)MoS_2, (b) WS_2 and (c) ReS_2 monolayers computed using PBE

Similar to MoS_2, WS_2 has a layered structure and electrical characteristics. When it changes smaller from bulk to monolayer, its electronic band gap transitions from an indirect (1.4 eV) to a direct (2 eV) transition. From above figure (b) the band gap of

WS_2 hexagonal monolayer is 1.8061 ev with the higher occupied level of -1.7971 ev and lower unoccupied level of 0.0090 ev.

Sefaattin Tongay et.al shows a comparison of the structure of a single layer of ReS2 with the conventional 1H structure of TMDs such as MoS_2. For ReS_2, DFT calculations show that the hexagonal (H) phase is unstable, whereas the octahedral (T) phase goes through the Peierls distortion, resulting in buckled S layers and zigzag Re chains along one of the lattice vectors in the plane. [139] Now ReS_2 hexagonal monolayer exhibit metallic property without band gap as shown in the figure (c) result from DFT calculation.

Band structure of MoS_2-WS_2

From recent studies show that MoS_2-WS_2 heterostructures' band gaps are usually between 1.0 and 2.0 electron volts (eV), which is perfect for absorbing most of the sun spectrum. For this specific study hetero structure MoS_2-WS_2 is semiconductor materials with direct band gab of 1.335eV.

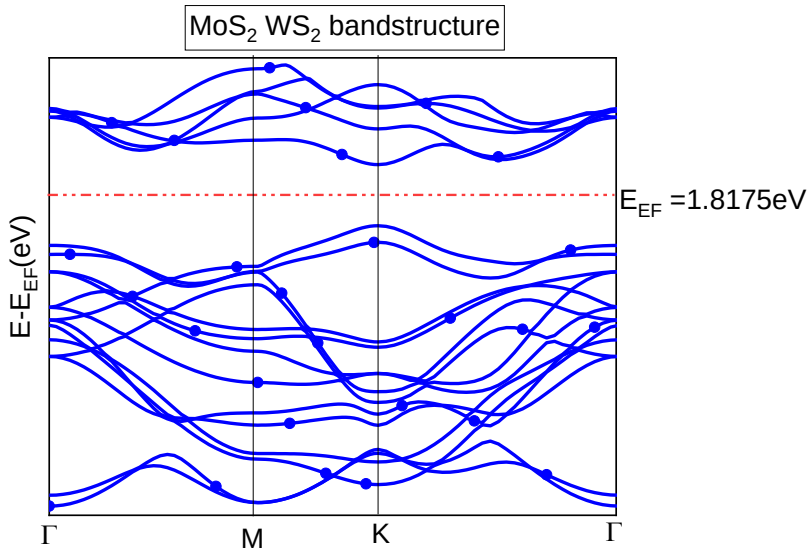

Figure 12 : MoS_2-WS_2 bandstructure

Research shows that light absorption has been enhanced for photocatalytic applications by combining MoS_2 and WS_2 as well as with other semiconductor materials to build heterostructures. These methods expand the range of light absorption by boosting surface area and active sites, improving charge separation, and raising MoS_2's efficiency in solar light.

Bandstructure of ReS_2-WS_2 and ReS_2-MoS_2

The formation of heterostructures combining MoS_2 (Molybdenum disulfide), WS_2 (Tungsten disulfide), and ReS_2 (Rhenium disulfide) represents an advanced strategy in the development of 2D semiconductor-based photocatalysts for water splitting. They can form type-II heterojunctions.

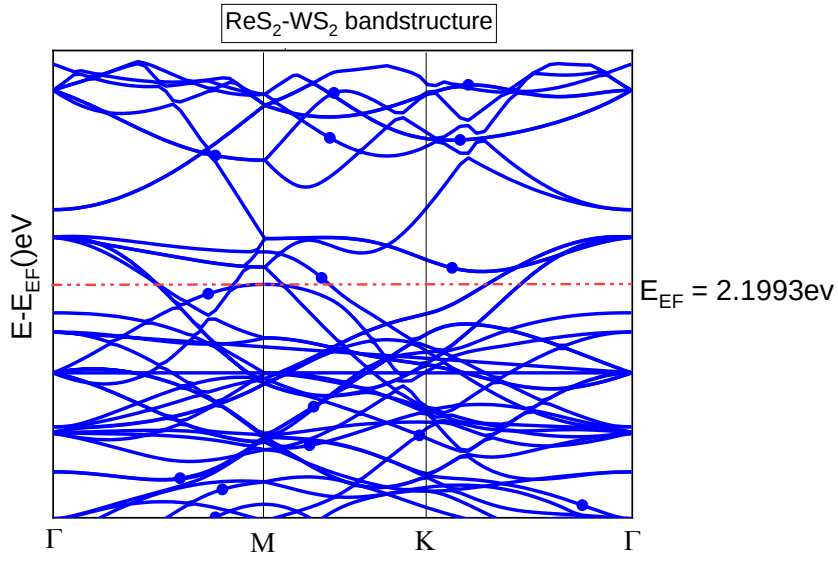

(a)

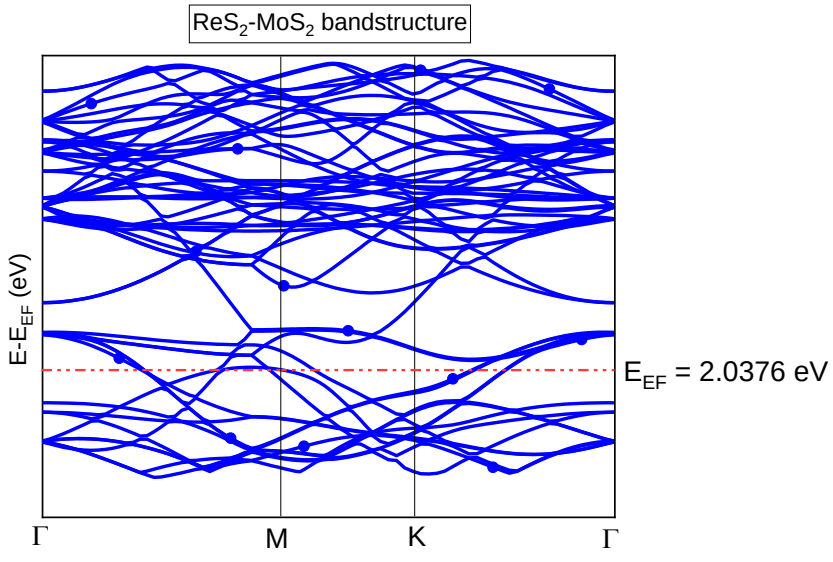

(b)

Figure 13 : (a) ReS_2-WS_2 (b) ReS_2-MoS_2 band structure.

The above band structure of hetero structure of ReS_2-WS_2 and ReS_2-MoS_2 has no band gap as we see in figure 13. In these junctions, the conduction band of one material overlap with the valence band of another, which facilitates efficient charge transfer. This alignment should helps in separating the electron-hole pairs more effectively to reducing recombination and increasing the photo catalytic activity.

From the DFT calculation we observe that the convergence parameters used for the band structure calculation, such as the K-point mesh and energy cutoff could influence the result and the band structure calculation is not fully converged, this may miss subtle features like a small band gap. Please note that also we have used PBE functionals due to computational resource limitation and in future work if hybrid functional is used like HSE we might get a small gap for the heterostructures.

Due to the bands overlapped and it became difficult to consider a band gap between conduction and valence band we obliged to try another phase of the monolayers rather than hexagonal phase for extra calculation and to meet this thesis objective.

Recent studies show that hetero-structure with no band gab are not favorable for water splitting studies, when we come to band edge analysis we consider phase change from hexagonal ReS_2 to triclinic phase to get semiconductor properties.

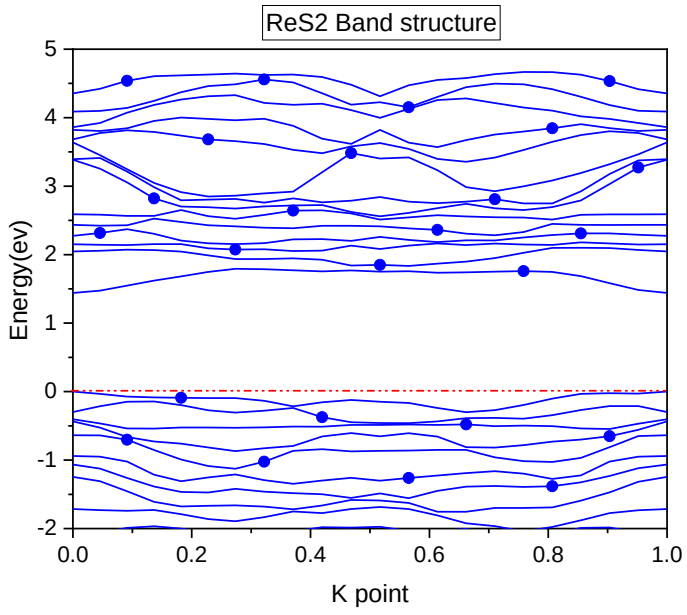

Figure 14 : Triclinic ReS_2 band structure.

4.2.2 Density of States (DOS)

The DOS, which stands for the energy level of the electrons, photons, or phonons in a solid crystal, is a characteristic that is widely utilized in quantum systems in condensed matter physics. In a quantum mechanical system, the electronic DOS measures how "packed" the electrons are in terms of energy levels. The DOS can range from zero at an energy level where the electrons cannot reach the material and occupy no space to a set occupancy value at a particular energy level where the electrons can access the material. The DOS is directly related to the idea of quantized energy levels, which is defined by quantum mechanics. [141]

DOS of Monolayer MoS2 , WS2 and ReS2

To investigate the electronic properties of MoS_2, WS_2 and ReS_2 monolayer systems, the density of states (DOSs) of the systems were calculated as shown in Figure 15. below

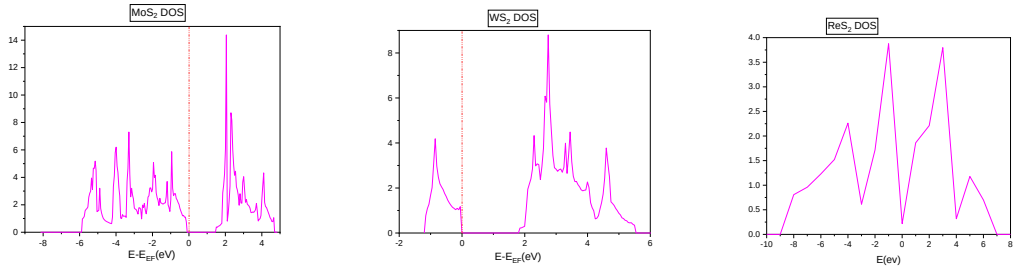

Figure 15: Density of states (DOSs) of the monolayer MoS_2, WS_2 and ReS_2 of monolayer systems. The Fermi energy (Ef) is set at zero and indicated by the vertical dotted black line.

DOS of Heterostructures

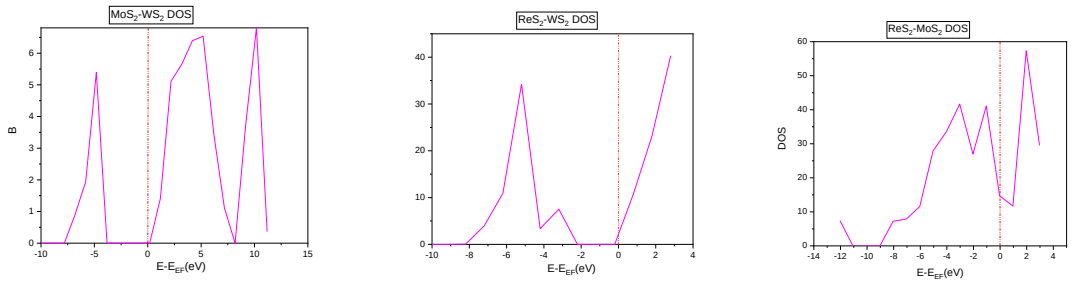

Figure 15 : Density of states (DOSs) of the monolayer (a) MoS_2-WS_2 (b) ReS_2-WS_2 (c) ReS_2-MoS_2 heterostructures. The Fermi energy (Ef) is set at zero and indicated by the vertical dotted black line.

The DOS value for plot a and b exhibit the structures are SC, which contradict the band structure plot above , this may be due to The DOS is an integrated quantity that sums contributions from all k points in the brillouin zone. This means it can show a band gap even if the gap is not present at the high-symmetry points visualized in the band structure. Band structure typically shows the energy dispersion of the electronic state in specific high-symmetry points of the brilouin zone.

In a hetero structure there may also be hybridization effect which is the two materials could lead to hybridization of electronic states. This can cause modification to the band structure at certain k-points, potentially making it appear as if there is no band gap. Meanwhile, the DOS, which is more comprehensive, could still capture the overall gap in the system.

4.3 Band Edge Alignment and Water Splitting Application

Two physical characteristics of semiconductor-based catalysts—the band gap and the band position—are crucial to the entire process. The energy of the generated exciton and the energy of the absorbed photon are determined by the band gap. In order to accomplish photocatalytic water splitting, semiconductors must fulfill the redox potentials of the H+/H2 and O2/H2O pairs with a minimum band gap of 1.23 eV. However, a higher band gap (>2.0 eV) is generally needed for the over potential associated with these phases in order to facilitate a smooth electron transfer process and the subsequent processes in hydrogen evolution. Simultaneously, the photocatalyst must possess a band gap that is small enough (Eg < 3.0 eV) to enable effective solar energy consumption. [142]

Conversely, the catalyst's redox potential is determined by the band location. In order to ensure that the proton reduction can be completed, an ideal conduction-band minimum for an effective single-component photocatalyst toward HER needs to be situated at a potential that is more negative than the electrochemical potential of HER.[143] [144]

Currently, MoS_2 is a class of TMDs with a band gap of 1.96 eV (direct) because of the

quantum confinement effect. This results in a MoS_2 monolayer with appropriate band positions and the capacity to absorb visible light, as Figure 8 [145, 146] illustrates.

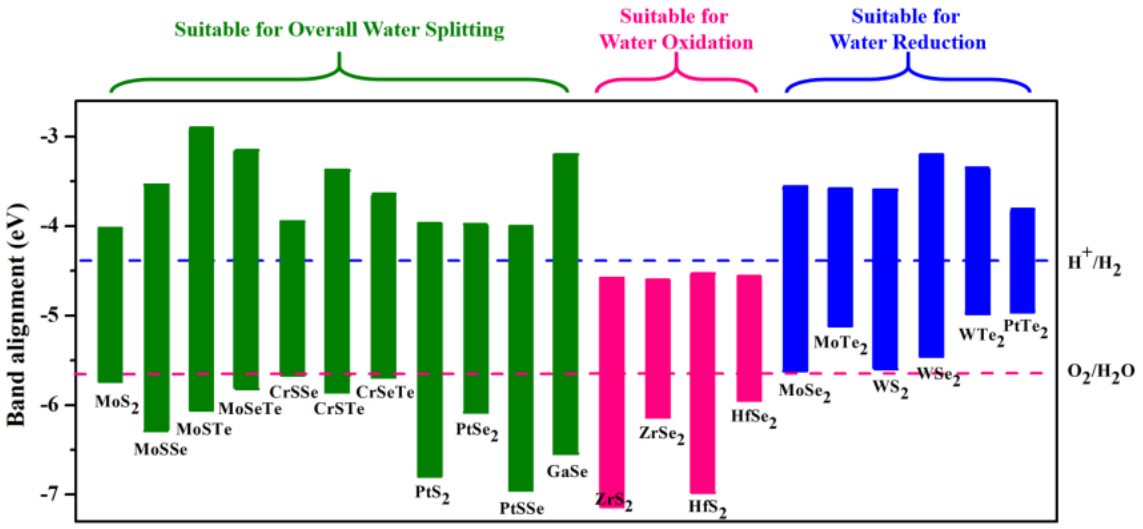

Figure 16. Band alignments of some typical 2D transition metal dichalcogenides with respect to the water reduction and oxidation potential for photocatalytic water splitting. The band alignments data are from references [147]

Three main phases make up the total photocatalytic water splitting reaction: [148]. (i) light absorption by a semiconductor to produce electron–hole pairs; (ii) charge separation and migration to the semiconductor surface; and (iii) surface reactions for the evolution of H_2 or O_2.

All three of the aforementioned processes' thermodynamic and kinetic balance influence the overall efficiency of photocatalytic water splitting. Significant work has been put into creating photocatalysts with efficient charge separation and migration (step ii) and wider absorption of the solar energy spectrum (step ii) during the last several decades. To improve the light absorption of wide-bandgap semiconductors, for example, a number of techniques have been used, including bandgap engineering (ion doping and solid solution formation), coupling with narrow-bandgap semiconductors, dye sensitization, surface plasmonic enhancement, and disorder engineering. [149]

The band edge alignment in heterosttructure materials is also important to evaluate their performance for water splitting applications. We have evaluated the band edge alignment of the two heterostructures as shown in figure 17. We can see from the plot both of the heterostructures have type II (staggered gap) which is very good for efficient separation of the photogenerated holes and electrons.

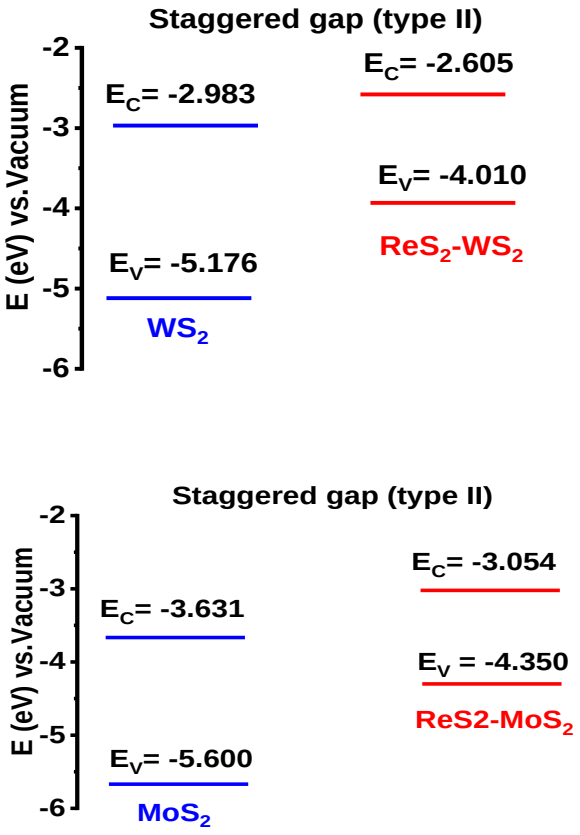

Figure 17 : Staggered gap

In addition we have plotted the band edge values of the monolayers and the heterostructure of table 4 together with the redox potential of water to evaluate the suitability of the structures for water splitting as shown in figure 18.

Table 4 band edge values

	Parameter cell a	Parameter cell c	Fermi level	VL	Work function	Band gap
ReS_2-MoS_2	6.43985	6.43985	2.51	1.5	5.306	1.405
ReS_2-WS_2	6.43995	6.43995	2.85	1.5	5.325	1.296
WS_2	3.18820	3.18820	4.03	1.46	5.417	2.129
MoS_2	3.18820	3.18820	3.58	2.02	5.597	1.964

We can observe that the CBM is higher than reduction potential of water for all the systems. This implies the system are a good material for hydrogen evolution reaction. However the VBM of the materials is not more negative than the oxidation potential of water and this implies the materials are not suitable for oxygen evolution reaction. So even if the systems are not suitable for over all water splitting they are very good material to produce hydrogen from water which is clean energy carrier.

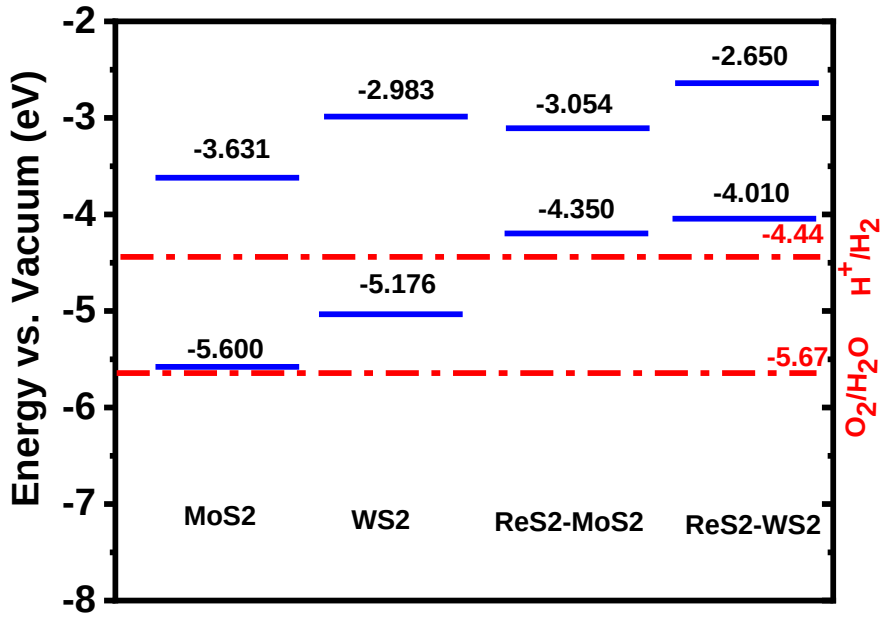

Figure 18 : Band edge of MoS_2 , WS_2 , ReS_2-MoS_2 & ReS_2-WS_2

4.4 Power Conversion Efficiency

4.4.1 Power Conversion Efficiency

Table 4 describes the photovoltaic efficiency of the specified hexagonal 2DTMD der Waals heterostructures with varying fill factor and potential loss. To determine the photovoltaic conversion efficiency, apply equations 12 through 15.[150],[151] For the material 2D TMD the highest power conversion efficiency is 22.06 percent, with a fill factor of 0.57 and a potential loss of 0.2 and 0.3.[152] [153]

Table 5 : photovoltaic efficiency

Compound	MoS_2	WS_2	MoS_2-WS_2
For potential loss = 0.3 and fill factor = 0.57			
Band gap	1.6804	1.8061	1.4536
PCE	17.45090333019244	15.993410953417026	19.73488185261373
For potential loss = 0.2 and fill factor = 0.57			
Band gap	1.6804	1.8061	1.4536
PCE	18.71509595110125247	17.055319920511977	21.445066772749357

$$\eta = \frac{\text{Voc x Jsc x FF}}{\text{Psun}} \qquad \text{equ 12}$$

where Voc (mV) is open circuit voltage, Jsc is short circuit current, FF is the fill factor, and Psun is solar power representing the total amount of incident solar radiation

$$eVoc = Eg - E\ loss \qquad \text{equ 13}$$

The band gap is denoted by Eg, the maximum short-circuit current density is denoted by Jsc, and Jsc is calculated using the NREL AM1.5 dataset.

$$J_{sc} = e\int_{Eg}^{\infty} \frac{SE}{E} d(E) \qquad \text{equ 14}$$

Psun is computed using the following equation

$$P_{Sun} = \int_{0}^{\infty} S(E)d(E) \qquad \text{equ 15}$$

The fill factors in this heterostructure we use 0.5 and 0.57, so we took this into account. For energy loss (Eloss), we use a value of 0.2 and 0.3.

The table 4 clearly illustrate that the power conversion efficiency of both the individual monolayers and the heterostructure exceeds 15%. This high level of efficiency is a key indicator of the potential of these materials in energy-related applications. Specifically, the materials investigated in this study demonstrate remarkable promise not only for hydrogen production through photocatalytic processes but also for broader green energy applications, such as in photovoltaic (solar cell) technologies.

Their ability to achieve a significant power conversion efficiency, coupled with an appropriate band gap, positions these materials as strong candidates for advancing renewable energy solutions. This aligns with the global push toward sustainable and environmentally friendly energy sources, further emphasizing the importance of continued research and development in this area. The findings of this study underscore the versatility and adaptability of these materials, highlighting their potential to contribute significantly to the transition to a cleaner energy future.

Chapter 5: Conclusion and Future work

5.1 Comparative Analysis

Table 6 : Comparative analysis

	Band gap	Photo-catalytic performance	ReSearcher's finding
MoS_2	1.6804 eV	Almost for overall water splitting reaction	MoS_2 = 1.46 eV [156]
WS_2	1.8061 eV	For hydrogen evolution reaction	WS_2 = 2.0 eV [157]
ReS_2-WS_2	1.296 eV	For hydrogen evolution reaction	ReS_2 = 1.44 eV [158]
ReS_2-MoS_2	1.405 eV	For hydrogen evolution reaction	MoS_2-WSe_2 =1.5 eV [159]

This study has investigated the potential of various two-dimensional materials and their heterostructures for applications in water splitting and photovoltaics. From the analysis, we conclude that MoS_2, with a band gap of 1.6804 eV, is nearly ideal for overall water splitting applications. On the other hand, WS_2, with a slightly larger band gap of 1.8061eV, is more suitable for hydrogen evolution reactions.

Furthermore,the heterostructures ReS_2-WS_2 and ReS_2-MoS_2 exhibit band gaps of 1.296eV and 1.405eV, respectively. These values with comparing their band edge alignment together with redox potential of water indicate their suitability for hydrogen evolution reaction as well. In addition to their potential in water-splitting applications, the individual monolayers and the heterostructures demonstrate promise for photovoltaic applications, with a power conversion efficiency exceeding 15%.

Overall, the findings highlight the versatility and effectiveness of these materials in advancing green energy technologies. By leveraging their unique properties, this work contributes to the ongoing efforts to develop sustainable and efficient energy solutions, underscoring the importance of continued exploration of 2D materials for energy-related applications.

5.2 Challenges and Future Work

As indicated in the title Investigation of 2D Hexagonal Transition Metal Dichalcogenide Heterostructures for Photocatalytic Water Splitting and Photovoltaic Solar Cells Using Density Functional Theory, during the DFT calculation it was somehow difficult to get bad gap for hexagonal phase of ReS_2 monolayer.

Due to semi metal properties of ReS_2 monolayer the heterostructure of ReS_2-MoS_2 and ReS_2-WS_2 characteristics is affected the band structure which is not stable. So another investigation was necessary to study photocatalytic water splitting and photovoltaic solar cells after adjusting the phase of ReS_2 monolayer from hexagonal to triclinic.

During the convergence test for heterostructures was challenging due to ambiguous and redundunt bad termination especially for relax calculation the super computer need huge storage due to lots of iteration done while the calculation is undertaken

I have suggest to future work more on formation, dynamics and recombination of interlayer excitons in ReS_2-WS_2 and ReS_2- MoS_2 heterostructures and investigate how temperature gradients and doping affect the performance of ReS_2

5.3 Recommendations

I have recommended to investigate how hetero structure interface affect the carrier life time and charge transfer process.

I have recommended research on DFT simulation to model the effect of various types of strain (uniaxial, biaxial or shear) on the electronic band gap, optical properties and phonon modes of hetero structure.

Future experimental and theoretical work directions will be on investigation the photo catalytic activity of ReS_2-WS_2 and ReS_2-MoS_2 hetero structure under different wavelength of light and studying the electrochemical properties of the hetero structure for energy storage application.

References

1. S. Pitchaimuthu, S. Marappan, V. Kharton, Materials for energy technologies: recent developments and trends, Mater. Lett. 253 (2019) 195.

2. Walter, M. G.; Warren, E. L.; McKone, J. R.; Boettcher, S. W.; Mi, Q. X.; Santori, E. A.; Lewis, N. S. Chem. Rev. 2010, 110, 6446-6473.
3. Abbasi, T.; Abbasi, S. Renewable Sustainable Energy Rev. 2011, 15, 3034-3040.
4. Bard, A. J.; Fox, M. A. Acc. Chem. Res. 1995, 28, 141-145.
5. Chu, S.; Majumdar, A. Nature 2012, 488, 294-303
6. Lewis, N. S. Science 2007, 315, 798-801.
7. Panwar, N.; Kaushik, S.; Kothari,S. Renewable Sustainable Energy Rev. 2011, 15, 1513-1524.
8. Solomon, B. D.; Krishna, K. Energy Policy 2011, 39, 7422-7431.
9. Solangi, K.; Islam, M.; Saidur, R.; Rahim, N.; Fayaz, H. Renewable Sustainable Energy Rev. 2011, 15, 2149-2163.
10. Xiaoyong Yang et.al, Recent Advancements and Future Prospects in Ultrathin 2D Semiconductor-Based Photocatalysts for Water Splitting, Catalysts 2020, 10, 1111; doi:10.3390/catal10101111]
11. Walter, M. G.; Warren, E. L.; McKone, J. R.; Boettcher, S. W.; Mi, Q. X.; Santori, E. A.; Lewis, N. S. Chem. Rev. 2010, 110, 6446-6473
12. Onyia, I.C.; Ezeonu, S.O.; Bessarabov, D.; Obodo, K.O. Density Functional Theory Studies of Transition Metal Doped Ti3N2 MXene Monolayer. *Comput. Mater. Sci.* 2021, *197*, 110613, doi:10.1016/J.COMMATSCI.2021.110613.
13. Beshir, B.T.; Obodo, K.O.; Asres, G.A. Janus Transition Metal Dichalcogenides in Combination with MoS2 for High-Efficiency Photovoltaic Applications: A DFT Study. *RSC Adv.* 2022, *12*, 13749–13755, doi:10.1039/D2RA00775D.
14. Obodo, K.O.; Ouma, C.N.M.; Obodo, J.T.; Gebreyesus, G.; Rai, D.P.; Ukpong, A.M.; Bouhafs, B. Sn3C2 Monolayer with Transition Metal Adatom for Gas Sensing: A Density Functional Theory Studies. *Nanotechnology* 2021, *32*, 355502, doi:10.1088/1361-6528/ac04d0.
15. Ouma, C.N.M.; Obodo, K.O.; Braun, M.; Amolo, G.O.; Bessarabov, D. Insights on Hydrogen Evolution Reaction in Transition Metal Doped Monolayer TcS2 from Density Functional Theory Calculations. *Appl. Surf. Sci.* 2019, *470*, 107–113, doi:10.1016/j.apsusc.2018.11.044.
16. Kuc, A.; Heine, T.; Kis, A. Electronic Properties of Transition-Metal Dichalcogenides. *Mrs Bull.* 2015, *40*, 577–584, doi:10.1557/mrs.2015.143.
17. Obodo, K.O.; Andrew, R.C.; Chetty, N. Modification of the Band Offset in Boronitrene. *Phys. Rev. B* 2011, *84*, 155308, doi:10.1103/PhysRevB.84.155308.
18. Obodo, J.T.; Obodo, K.O.; Schwingenschlögl, U. Negative Differential Conductance in TwoDimensional C-Functionalized Boronitrene. *New J. Phys.* 2015, *17*, 93012, doi:10.1088/1367- 2630/17/9/093012.
19. Obodo, K.O.; Chetty, N.; Obodo, J.T. Band Offset Engineering in C-Functionalized Boronitrene. *Comput. Mater. Sci.* 2017, *128*, 373–378, doi:10.1016/j.commatsci.2016.11.046.

20. Jiang, J.; Ling, C.; Xu, T.; Wang, W.; Niu, X.; Zafar, A.; Yan, Z.; Wang, X.; You, Y.; Sun, L.;et al. Defect Engineering for Modulating the Trap States in 2D Photoconductors. *Adv. Mater.* 2018, *30*, 1804332(1-6), doi:10.1002/adma.201804332.
21. Huang, J.; Gao, H.; Xia, Y.; Sun, Y.; Xiong, J.; Li, Y.; Cong, S.; Guo, J.; Du, S.; Zou, G. Enhanced Photoelectrochemical Performance of Defect-Rich ReS2 Nanosheets in VisibleLight Assisted Hydrogen Generation. *Nano Energy* 2018, *46*, 305–313, doi:10.1016/j.nanoen.2018.02.003.
22. Walter, M.G.; Warren, E.L.; McKone, J.R.; Boettcher, S.W.; Mi, Q.; Santori, E.A.; Lewis, N.S. Solar water splitting cells. *Chem. Rev.* 2010, *110*, 6446–6473
23. Inoue, T.; Fujishima, A.; Konishi, S.; Honda, K. Photoelectrocatalytic reduction of carbon dioxide in aqueous suspensions of semiconductor powders. Nature 1979, 277, 637-638
24. Chen, X. B.; Shen, S. H.; Guo, L. J.; Mao, S. S. Semiconductorbased Photocatalytic Hydrogen Generation. Chem. Rev. 2010, 110,
25. Leng, M.; Chen, Y.; Xue, J. M. Synthesis of TiO2 nanosheets via an exfoliation route assisted by a surfactant. Nanoscale 2014, 6, 8531-8534.
26. Bao, N.; Shen, L.; Takata, T.; Domen, K.; Gupta, A.; Yanagisawa, K.; Grimes, C. A. Facile cd-thiourea complex thermolysis synthesis of phase-controlled CdS nanocrystals for photocatalytic hydrogen production under visible light. J. Phys. Chem. C 2007, 111, 17527-17534.
27. Ng, Y. H.; Iwase, A.; Kudo, A.; Amal, R. Reducing Graphene Oxide on a Visible-Light BiVO4 Photocatalyst for an Enhanced Photoelectrochemical Water Splitting. J. Phys. Chem. Lett. 2010, 1, 2607-2612
28. Kudo, A.; Miseki, Y. Heterogeneous photocatalyst materials for water splitting. Chem. Soc. Rev. 2009, 38, 253-278.
29. Wenchao Peng et.al, Roles of Two-Dimensional Transition Metal Dichalcogenides as Cocatalysts in Photocatalytic Hydrogen Evolution and Environmental Remediation , DOI: 10.1021/acs.iecr.7b00371 Ind. Eng. Chem. Res. 2017, 56, 4611-4626
30. Jingrun Ran et.al , Earth-abundant cocatalysts for semiconductorbased photocatalytic water splitting, *Chem. Soc. Rev.*, 2014, 43, 7787
31. A. Kudo, Y. Miseki, Chem. Soc. Rev. 38 (2009) 253–278
32. Uttam Gupta, C.N.R. Rao, Hydrogen generation by water splitting using MoS2 and other transition metal dichalcogenides, Nano Energy 41 (2017) 49-65
33. A. Chaves, J. G. Azadani, H. Alsalman, D. R. da Costa, R. Frisenda, A. J.Chaves, S. H. Song, Y. D. Kim, D. He, J. Zhou, A. Castellanos-Gomez, F. M. Peeters, Z. Liu, C. L. Hinkle, S. H. Oh, P. D. Ye, S. J. Koester, Y. H Lee, P. Avouris, X. Wang and T. Low, *npj 2D Mater. Appl.*, 2020, 4(1),
34. A. Nijamudheen and A. v. Akimov, J. Phys. Chem. C, 2017, 121, 6520–6532
35. Obodo, K.O.; Ouma, C.N.M.; Bessarabov, D. Low-Temperature Water Electrolysis. In *POWER TO FUEL: HOW TO SPEED UP A HYDROGEN ECONOMY*; Spazzafumo, G., Ed.; Elsevier: North Holland, 2021; pp. 1–287.
36. [Yang, X., Singh, D., & Ahuja, R. (2020). *Recent Advancements and Future Prospects in Ultrathin 2D Semiconductor-Based Photocatalysts for Water Splitting. Catalysts, 10(10), 1111.* doi:10.3390/catal10101111]

37. Alfaifi, B.Y.; Ullah, H.; Alfaifi, S.; Tahir, A.A.; Mallick, T.K. Photoelectrochemical Solar Water Splitting: From Basic Principles to Advanced Devices. *Veruscript Funct. Nanomater*. 2018, *2*, BDJOC3, doi:10.22261/fnan.bdjoc3

38. Xiaoyong Yang et.al. Recent Advancements and Future Prospects in Ultrathin 2D Semiconductor-Based Photocatalysts for Water Splitting, Catalysts 2020, 10, 1111; doi:10.3390/catal10101111

39. Dean CR, Young AF, Meric I, et al. Boron nitride substrates for high-quality graphene electronics. Nat Nanotechnol 2010; 5: 722–726.
40. Geim AK, Grigorieva IV. Van der Waals heterostructures. Nature 2013; 499: 419–425.
41. Wang H, Liu F, Fu W, et al. Two-dimensional heterostructures: fabrication, characterization, and application. Nanoscale 2014; 6: 12250–12272
42. Lin YC, Ghosh RK, Addou R, et al. Atomically thin resonant tunnel diodes built from synthetic van der Waals heterostructures. Nat Commun 2015; 6:7311
43. Chen H, Wen X, Zhang J, et al. Ultrafast formation of interlayer hot excitons in atomically thin MoS2/WS2 heterostructures. Nat Commun 2016; 7: 12512
44. Roy T, Tosun M, Cao X, et al. Dual-Gated MoS2/WSe2 van der Waals tunnel diodes and transistors. ACS Nano 2015; 9: 2071–2079.
45. Furchi MM, Pospischil A, Libisch F, et al. Photovoltaic effect in an electrically tunable van der Waals heterojunction. Nano Lett 2014; 14: 4785-4791.
46. Priyanka Gangulyet.al, 2D Nanomaterials for Photocatalytic Hydrogen Production, ACS Energy Lett. 2019, 4, 1687-1709
47. Aman kassaye Sibhatu et.al. DFT investigation of the electronic and optical properties of hexagonal MX2/ZrXO (M = W, Mo and X = S, Se) van der Waals heterostructures for photovoltaic solar cell application, *27th October 2022*
48. Akanksha Urade ,What are Transition Metal Dichalcogenides (TMDs), https://www.azonzno.com/aothors/akanksha-akanksha, Feb 7 2022

49. Kyungnam Kang et.al, Synthesis, Modelling and Characterization of 2D Materials and their Heterostructures, DOI: https://doi.org/10.1016/B978-0-12-818475-2.00012-X
50. H.J. Conley, B. Wang, J.I. Ziegler, R.F. Haglund, S.T. Pantelides, K.I. Bolotin, Bandgap engineering of strained monolayer and bilayer MoS2, Nano Lett. 13 (8) (2013) 36263630.
51. W. Zhao, et al., Evolution of electronic structure in atomically thin sheets of WS2 and WSe2, ACS Nano 7 (1) (2013) 791797.
52. A. Arora, M. Koperski, K. Nogajewski, J. Marcus, C. Faugeras, M. Potemski, Excitonic resonances in thinfilms of WSe2: from monolayer to bulk material, Nanoscale 7 (23) (2015) 1042110429.
53. M.M. Ugeda, et al., Giant bandgap renormalization and excitonic effects in a monolayer transition metaldichalcogenide semiconductor, Nat. Mater. 13 (12) (2014) 10911095. The type II heterojunction can be easily fabricated with TMDs due to their band alignment [8-10.

54. X. Li, H. Zhu, Two-dimensional MoS2: properties, preparation, and applications, J. Mater. 1 (1) (2015) 3344] The TMD monolayer has two inequivalent valleys (K and 2 K valley) at the corner of a Brillouin zone due to inversion symmetry breaking
55. H. Zeng, J. Dai, W. Yao, D. Xiao, X. Cui, Valley polarization in MoS2 monolayers by optical pumping, Nat. Nanotechnol. 7 (8) (2012) 490493.] The strong spinorbit coupling and inequivalent valleys lead valley dependent optical selection rule and spinvalley locking
56. D. Xiao, G.-B. Liu, W. Feng, X. Xu, W. Yao, Coupled spin and valley physics in monolayers of MoS2 and other group-VI dichalcogenides, Phys. Rev. Lett. 108 (19) (2012) 196802
57. K.F. Mak, C. Lee, J. Hone, J. Shan, T.F. Heinz, Atomically thin MoS2: A new direct-gap semiconductor,Phys. Rev. Lett. 105 (13) (2010) 25
58. Melinda Mohl et.al, 2D Tungsten Chalcogenides: Synthesis, Properties and Applications, www.advmatinterfaces.de , www.advancedsciencenews.com
59. Jesse D. Benck et.al, Catalyzing the Hydrogen Evolution Reaction (HER) with Molybdenum Sulfide Nanomaterials, dx.doi.org/10.1021/cs500923c | ACS Catal. 2014, 4, 3957-3971
60. L. Liao, et al., MoS2 formed on mesoporous graphene as a highly active catalyst for hydrogen evolution, Adv. Funct. Mater. 23 (42) (2013) 5326e5333.
61. Rapoport, L.; Fleischer, N.; Tenne, R. J. Mater. Chem. 2005, 15, 1782–1788
62. Abotsi, G. M.; Scaroni, A. W. Fuel Process. Technol. 1989, 22, 107–133
63. Jaramillo, T. F.; Jørgensen, K. P.; Bonde, J.; Nielsen, J. H.; Horch, S.; Chorkendorff, I. Science 2007, 317, 100–102].
64. Z. Deng et al., Synthesized ultrathin MoS2 nanosheets perpendicular to graphene for catalysis of hydrogen evolution reaction, Chem. Commun. 51 (10) (2015) 1893–1896
65. M.A. Lukowski, A.S. Daniel, F. Meng, A. Forticaux, L. Li, S. Jin, Enhanced hydrogen evolution catalysis from chemically exfoliated metallic MoS2 nanosheets, J. Am. Chem. Soc. 135 (2013) 1027410277.
66. Y. Jiang, et al., Reduced graphene oxide-modified carbon nanotube/polyimide film supported MoS2 nanoparticles for electro catalytic hydrogen evolution, Adv. Funct. Mater. 25 (18) (2015) 2693-2700.
67. J. Guo et al., Oxygen-incorporated MoS2 ultrathin nanosheets grown on graphene for efficient electrochemical hydrogen evolution, J. Power Sources 291 (2015), 195–200.
68. Y. Yu, S.-Y. Huang, Y. Li, S.N. Steinmann, W. Yang, L. Cao, Layer-dependent electrocatalysis of MoS2 for hydrogen evolution, Nano Lett. 14 (2014) 553558.
69. D. Voiry, H. Yamaguchi, J. Li, R. Silva, D.C.B. Alves, T. Fujita, et al., Enhanced catalytic activity in strained chemically exfoliated WS2 nanosheets for hydrogen evolution, Nat. Mater. 12 (2013) 850855.
70. P.D. Tran, S.Y. Chiam, P.P. Boix, Y. Ren, S.S. Pramana, J. Fize, et al., Novel cobalt/nickel-tungstensulfide catalysts for electrocatalytic hydrogen generation from water, Energy Environ. Sci. 6 (2013) 24522459.
71. S. Tongay, H. Sahin, C. Ko, A. Luce, W. Fan, K. Liu, J. Zhou, Y.-s. Huang, C.-h. Ho, J. Yan, D. F. Ogletree, S. Aloni, J. Ji, S. Li, J. Li, F. M. Peeters and J. Wu, Nature Communications, 2014, 5, 1–6.

72. A. Thamizhavel, M. Chhowalla, M. Deshmukh and A. Bhattacharya, Chemistry of Materials, 2016, 28, 3352–3359
73. E. Lorchat, G. Froehlicher and S. Berciaud, ACS nano, 2016, 10, 2752–2760.
74. Y. C. Cheng, Z. Y. Zhu, W. B. Mi, Z. B. Guo and U. Schwingenschlögl, Physical Review B - Condensed Matter and Materials Physics, 2013, 87, 2–5
75. J.-K. Qin, W.-Z. Shao, C.-Y. Xu, Y. Li, D.-D. Ren, X.-G. Song and L. Zhen, ACS Applied Materials and Interfaces, 2017, 9, 15583–15591
76. James, B. D., Baum, G. N., Perez, J. & Baum, K. N. Technoeconomic Analysis of Photoelectrochemical (PEC) Hydrogen Production. Report No. GS-10F-009J, published on U.S. DOE EERE website.www1.eere.doe.gov/hydrogenandfuelcells/ pdfs/pec_technoeconomic_analysis.pdf (US Department of Energy, 2009).
77. Ashcroft, A. T., Cheetham, A. K., Green, M. L. H. & Vernon, P. D. F. Partial oxidation of methane to synthesis gas-using carbon-dioxide. Nature 352,991)
78. Cortright, R. D., Davda, R. R. & Dumesic, J. A. Hydrogen from catalytic reforming of biomass-derived hydrocarbons in liquid water. Nature 418, 964-967 (2002).
79. Rostrup-Nielsen, J. R., Sehested, J. & Norskov, J. K. in Advances in Catalysis Vol. 47 (eds Gates, B. C. & Knozinger, H.) 65–139 (2002).
80. Joo, S. H. et al. Ordered nanoporous arrays of carbon supporting high dispersions of platinum nanoparticles. Nature 412, 169–172 (2001).
81. Si, Y. C. & Samulski, E. T. Exfoliated graphene separated by platinum nanoparticles. Chem. Mater. 20, 6792–6797 (2008).
82. Sheng, W. C., Gasteiger, H. A. & Shao-Horn, Y. Hydrogen oxidation and evolution reaction kinetics on platinum: acid vs alkaline electrolytes. J. Electrochem. Soc. 157, B1529–B1536 (2010).
83. Khaselev, O. & Turner, J. A. A monolithic photovoltaic-photoelectrochemical device for hydrogen production via water splitting. Science 280, 425–427(1998).
84. E. Kabir, P. Kumar, S. Kumar, A. A. Adelodun and K. H. Kim, *Renewable Sustainable Energy Rev.*, 2018, 82, 894–900 CrossRef .
85. B. Parida, S. Iniyan and R. Goic, *Renewable Sustainable Energy Rev.*, 2011, 15, 1625–1636 CrossRef CAS .
86. J. Gallagher, Heterogeneous catalysis: how heteroatom-doped graphenes make hydrogen faster, Nat. Rev. Chem. 2 (2018) 0138.
87. Hinnemann, B.; Moses, P. G.; Bonde, J.; Jørgensen, K. P.; Nielsen, J. H.; Horch, S.; Chorkendorff, I.; Nørskov, J. K. Biomimetic hydrogen evolution: MoS2 nanoparticles as catalyst for hydrogen evolution. J. Am. Chem. Soc. 2005, 127 (15), 5308-5309
88. Onyia, I.C.; Ezeonu, S.O.; Bessarabov, D.; Obodo, K.O. Density Functional Theory Studies of Transition Metal Doped Ti3N2 MXene Monolayer. *Comput. Mater. Sci.* 2021, *197*, 110613, doi:10.1016/J.COMMATSCI.2021.110613.
89. Beshir, B.T.; Obodo, K.O.; Asres, G.A. Janus Transition Metal Dichalcogenides in Combination with MoS2 for High-Efficiency Photovoltaic Applications: A DFT Study. *RSC Adv.* 2022, *12*, 13749–13755, doi:10.1039/D2RA00775D.
90. Obodo, K.O.; Ouma, C.N.M.; Obodo, J.T.; Gebreyesus, G.; Rai, D.P.; Ukpong, A.M.; Bouhafs, B. Sn3C2 Monolayer with Transition Metal Adatom for Gas Sensing: A Density Functional Theory Studies. *Nanotechnology* 2021, *32*, 355502, doi:10.1088/1361-6528/ac04d0.

91. Zhou, X.; Liu, N.; Schmidt, J.; Kahnt, A.; Osvet, A.; Romeis, S.; Zolnhofer, E. M.; Marthala, V. R. R.; Guldi, D. M.; Peukert, W.; et al. Noble-Metal-Free Photocatalytic Hydrogen Evolution Activity: The Impact of Ball Milling Anatase Nanopowders with TiH2. Adv. Mater. 2017, 29 (5), 1604747.
92. [F] Priyanka Ganguly et.al, 2D Nanomaterials for Photocatalytic Hydrogen Production, ACS Energy Lett. 2019, 4, 1687-1709
93. E. Kabir, P. Kumar, S. Kumar, A. A. Adelodun and K. H. Kim, *Renewable Sustainable Energy Rev.*, 2018, 82, 894–900 CrossRef .
94. B. Parida, S. Iniyan and R. Goic, *Renewable Sustainable Energy Rev.*, 2011, 15, 1625–1636 CrossRef CAS .
95. J. Gallagher, Heterogeneous catalysis: how heteroatom-doped graphenes make hydrogen faster, Nat. Rev. Chem. 2 (2018) 0138.
96. Wang, Q.; Hisatomi, T.; Jia, Q.; Tokudome, H.; Zhong, M.; Wang, C.; Pan, Z.; Takata, T.; Nakabayashi, M.; Shibata, N.; et al. Scalable water splitting on particulate photocatalyst sheets with a solar-to-hydrogen energy conversion efficiency exceeding 1%. *Nat. Mater.* 2016, *15*, 611–615.
97. Kuc, A.; Heine, T.; Kis, A. Electronic Properties of Transition-Metal Dichalcogenides. *Mrs Bull.* 2015, *40*, 577–584, doi:10.1557/mrs.2015.143.
98. B. Parida, S. Iniyan and R. Goic, *Renewable Sustainable Energy Rev.*, 2011, 15, 1625–1636 CrossRef CAS .
99. Teoh, W.; Scott, J.; Amal, R. Progress in Heterogeneous Photocatalysis: From Classical Radical Chemistry to Engineering Nanomaterials and Solar Reactors. J. Phys. Chem. Lett. 2012, 3 (5), 629-639
100. She, X.; Wu, J.; Xu, H.; Zhong, J.; Wang, Y.; Song, Y.; Nie, K.; Liu, Y.; Yang, Y.; Rodrigues, M.T.F.; et al. High efficiency photocatalytic water splitting using 2D *a*-Fe2O3/*g*-C3N4 Z-scheme catalysts. *Adv. Energy Mater.* 2017, *7*, 1700025]
101. Walter, M. G.; Warren, E. L.; McKone, J. R.; Boettcher, S. W.; Mi, Q. X.; Santori, E. A.; Lewis, N. S. Chem. Rev. 2010, 110, 6446-6473.
102. Bing Han & Yun Hang Hu, MoS 2 as a co-catalyst for photocatalytic hydrogen production from water, © 2016 The Authors. *Energy Science & Engineering*
103. Rindt, C. C. M., & Gaastra-Nedea, S. V. (2015). *Modeling thermochemical reactions in thermal energy storage systems. Advances in Thermal Energy Storage Systems, 375–415.* doi:10.1533/9781782420965.3.3
104. Chaoliang Tan et.al, Recent Advanced in Ultrathin Two- Dimentional Nanomaterials, DOI: 10.1021/acs.chemrev.6b00558 Chem. Rev. 2017, 117, 6225-6331]
105. Shanmugam, M.; Jacobs-Gedrim, R.; Song, E. S.; Yu, B. TwoDimensional Layered Semiconductor/Graphene Heterostructures for Solar Photovoltaic Applications. Nanoscale 2014, 6, 12682-12689
106. J. Gallagher, Heterogeneous catalysis: how heteroatom-doped graphenes make hydrogen faster, Nat. Rev. Chem. 2 (2018) 0138.
107. B. Hinnemann, P.G. Moses, J. Bonde, K.P. Jørgensen, J.H. Nielsen, S. Horch, et al., Biomimetic hydrogen evolution: MoS2 nanoparticles as catalyst for hydrogen evolution, J. Am. Chem. Soc. 127 (2005) 53085309

108. Mak KF, Lee C, Hone J, et al. Atomically thin MoS2: a new direct-gap semiconductor. Phys Rev Lett 2010; 105: 136805
109. Splendiani A, Sun L, Zhang Y, et al. Emerging photoluminescence in monolayer MoS2. Nano Lett 2010; 10: 1271–1275
110. T.F. Jaramillo, K.P. Jørgensen, J. Bonde, J.H. Nielsen, S. Horch, I. Chorkendorff, Identification of active edge sites for electrochemical H2 evolution from MoS2 nanocatalysts, Sci. 317 (2007) 100102.
111. A. Kuc, T. Heine, The electronic structure calculations of two-dimensional transition-metal dichalcogenides in the presence of external electric and magnetic fields, Chem. Soc. Rev. 44 (2015) 26032614.
112. Lv, R. et al., (2015) Twodimensional transition metal dichalcogenides: Clusters, ribbons, sheets and more. *Nano Today*, 10(5), pp.559–592. https://www.sciencedirect.com/science/article/pii/S1748013215000961
113. M.J. Armstrong, C. O'Dwyer, W.J. Macklin, J.D. Holmes, Evaluating the performance of nanostructured materials as lithium-ion battery electrodes, Nano Res. 7 (1) (2014).
114. K. Leng, et al., Phase restructuring in transition metal dichalcogenides for highly stable energy storage, ACS Nano 10 (10) (2016)
115. H. Jiang, et al., 2D monolayer MoS2-carbon interoverlapped superstructure: engineering ideal atomic interface for lithium ion storage, Adv. Mater. 27 (24) (2015) 36873695
116. P. Liu, B. Xiang, 2D hetero-structures based on transition metal dichalcogenides: fabrication, properties and applications, Science Bulletin (2017), doi:http://dx.doi.org/10.1016/j.scib.2017.08.007
117. Morasae Samad et.al, Group 6 transition metal dichalcogenide nanomaterials: synthesis, applications and future perspectives, *Nanoscale Horiz.*, 2018, 3, 90
118. Obodo, K.O.; Ouma, C.N.M.; Modisha, P.M.; Bessarabov, D. Density Functional Theory Calculation of Ti3C2 MXene Monolayer as Catalytic Support for Platinum towards the Dehydrogenation of Methylcyclohexane. *Appl. Surf. Sci.* 2020, *529*, 147186, doi:10.1016/j.apsusc.2020.147186
119. Cao, Z.; Harb, M.; Lardhi, S.; Cavallo, L. Impact of interfacial defects on the properties of monolayer transition metal dichalcogenide lateral heterojunctions. J. Phys. Chem. Lett. 2017, 8 (7), 1664- 1669.
120. P. A, Z. V.A, B. L.L, A multiple-item scale for measuring consumer perceptions of service quality, J. Retail. 64 (1998) 12–40
121. K. Hohenberg, Inhomogeneous Electron Gas, Phys. Rev. 155 (1964) B864–B871.
122. Kohn W. Sham L. J., Self-Consistent Equations Including Exchange and Correlation Effects, Phys. Rev. 140 (1965) A1133–A1138.

123. Perdew, J.P.; Burke, K.; Ernzerhof, M. Generalized Gradient Approximation Made Simple.*Phys. Rev. Lett.* 1996, *77*, 3865(4).

124. Tkatchenko, A.; Scheffler, M. Accurate Molecular van Der Waals Interactions from GroundState Electron Density and Free-Atom Reference Data. *Phys. Rev. Lett.* 2009, *102*, 073005, doi:10.1103/PhysRevLett.102.073005.

125. Rindt, C. C. M., & Gaastra-Nedea, S. V. (2015). *Modeling thermochemical reactions in thermal energy storage systems. Advances in Thermal Energy Storage Systems, 375–415.* doi:10.1533/9781782420965.3.3

126. A. Hossain, Introduction to density functional theory, 1 (2004) 1–7. https://doi.org/10.1007/s00214-013-1372-6.

127. Stephen J. Klippensteina and Carlo Cavallotti, Ab initio kinetics for pyrolysis and combustion systems, Computer-Aided Chemical Engineering, Volume 45, ISSN 1570-7946, https://doi.org/10.1016/B978-0-444-64087-1.00002-4

128. M.A. Lukowski, A.S. Daniel, F. Meng, A. Forticaux, L. Li, S. Jin, Enhanced hydrogen evolution catalysis from chemically exfoliated metallic MoS2 nanosheets, J. Am. Chem. Soc. 135 (2013) 1027410277.

129. B.T. Beshir, K.O. Obodo, Janus transition metal dichalcogenides in combination with MoS2 for high-e ffi ciency photovoltaic applications : a DFT study †, (2022) 13749–13755. https://doi.org/10.1039/d2ra00775d.

130. S. Saini, A. Shrivastava, A. Dixit, S. Singh, Ultra-low lattice thermal conductivity and high figure of merit for Janus MoSeTe monolayer: a peerless material for high temperature regime thermoelectric devices, J. Mater. Sci. 57 (2022) 7012–7022. https://doi.org/10.1007/s10853-022-07065-3.

131. Xiaoyong Yang et.al. Recent Advancements and Future Prospects in Ultrathin 2D Semiconductor-Based Photocatalysts for Water Splitting, Catalysts 2020, 10, 1111; doi:10.3390/catal10101111

132. A. Zunger, J. Phys. C 7, 96 (1974).
133. R. A. Evarestov, Phys. Status Solidi B 72, 569 (1975).
134. S. G. Louie and M. L. Cohen, Phys. Rev. Lett. 35, 866 (1975).
135. Voicu Popescu and Alex Zunger, Extracting E versus k effective band structure from supercell calculations on alloys and impurities, ©2012 American Physical Society DOI: 10.1103/PhysRevB.85.085201
136. E.A. Peterson, T.T. Debela, G.M. Gomoro, J.B. Neaton, G.A. Asres, Electronic structure of strain-tunable Janus WSSe-ZnO heterostructures from first-principles, RSC Adv. 12 (2022) 31303–31316. https://doi.org/10.1039/d2ra05533c
137.
138. 141 T. B. Boykin, N. Kharche, G. Klimeck, and M. Korkusinski, J. Phys.: Condens. Matter 19, 036203 (2007)
139. K.F. Mak, C. Lee, J. Hone, J. Shan, T.F. Heinz, Atomically thin MoS2: A new direct-gap semiconductor,Phys. Rev. Lett. 105 (13) (2010) 25.]
140. H.J. Conley, B. Wang, J.I. Ziegler, R.F. Haglund, S.T. Pantelides, K.I. Bolotin, Bandgap engineering of strained monolayer and bilayer MoS2, Nano Lett. 13 (8) (2013) 36263630.

141. Sefaattin Tongay et.al , Monolayer behaviour in bulk ReS2 due to electronic and vibrational decoupling , 10.1038/ncomms4252 , www.nature.com/naturecommunications
142. Aman kassaye Sibhatu et.al. DFT investigation of the electronic and optical properties of hexagonal MX2/ZrXO (M = W, Mo and X = S, Se) van der Waals heterostructures for photovoltaic solar cell application, *27th October 2022*

143. Marchiori, R. (2017). Mathematical Fundamentals of Nanotechnology. Nanostructures, 209–232. doi:10.1016/b978-0-323-49782-4.00008-5
144. Y. Qu , X. Duan , *Chem. Soc. Rev.* 2013, *42*, 2568
145. M. G. Walter , E. L. Warren , J. R. McKone , S. W. Boettcher , Q. Mi , E. A. Santori , N. S. Lewis , *Chem. Rev.* 2010, *110*, 6446
146. *Qipeng Lu et.al, 2D Transition-Metal-Dichalcogenide-Nanosheet-Based Composites for Photocatalytic and Electrocatalytic Hydrogen Evolution Reactions, Adv. Mater. 2016, 28, 1917–1933*
147. Kibsgaard , T. F. Jaramillo , F. Besenbacher , *Nat. Chem.* 2014, *6*, 248 .
148. M. A. Lukowski , A. S. Daniel , F. Meng , A. Forticaux , L. Li , S. Jin , *J. Am. Chem. Soc.* 2013, *135*, 10274
149. K. Lai, C. L. Yan, L. Q. Gao and W. B. Zhang, J. Phys. Chem. C, 2018, 122, 7656–7663
150. . Fujishima and K. Honda, Nature, 1972, 238, 37 7787

151. Peng, R.; Ma, Y.; Huang, B.; Dai, Y. Two-dimensional Janus PtSSe for photocatalytic water splitting under the visible or infrared light. *J. Mater. Chem. A* 2019, *7*, 603–610
152. P. K. Nayak, S. Mahesh, H. J. Snaith and D. Cahen, Nat. Rev. Mater., 2019, 4, 269–285
153. M. R. Filip, C. Verdi and F. Giustino, J. Phys. Chem. C, 2015, 119, 25209–25219.

154. M. M. Furchi, F. Höller, L. Dobusch, D. K. Polyushkin, S. Schuler and T. Mueller, npj 2D Mater. Appl., 2018, 2(1), 1–7
155. Jingrun Ran et.al , Earth-abundant cocatalysts for semiconductorbased photocatalytic water splitting, Chem. Soc. Rev., 2014, 43,
156. Jacob WESTHOLM, First principles calculations of 2D materials, Uppsala University, Department of Physics and Astronomy, June 25, 2018
157. Paracchino, A., Laporte, V., Sivula, K., Grätzel, M. & Thimse, E. Highly active oxide photocathode for photoelectrochemical water reduction. Nature Mater. 10, 456–461 (2011).
158. Dr. Y. Xiong,et.al , Electronic and Optoelectronic Applications Based on ReS2, State Key Laboratory of ASIC and System ,School of Microelectronics, 2019

159. Cao, Z.; Harb, M.; Lardhi, S.; Cavallo, L. Impact of interfacial defects on the properties of monolayer transition metal dichalcogenide lateral heterojunctions. J. Phys. Chem. Lett. 2017, 8 (7), 1664- 1669.